

Methods and results of application of the neutron diffractometry in the Earth sciences: A Review

A. N. Nikitin and T. I. Ivankina

Frank Laboratory of Neutron Physics Joint Institute of Nuclear Research Dubna, Moscow Region

Abstract. Fundamental advantages of the neutron methods, that are based on the phenomenal properties of the neutron allow to extend the number of problems to be resolved in the solid-state physics, in geology and in geophysics, are analyzed in detail. A definition is given in the review to the crystallographic textures and emphasis was placed on the fact that the preferred orientation of the crystal lattices of the rock forming minerals as one of the main factors that controls the rock anisotropy, is an inherited property, acquired as a result of magmatism and metamorphism and other processes that governed the Earth's lithosphere formation. New results of investigation of the rock textural regularities and hence peculiarities of physical properties, such as behavior and anisotropy of the elastic wave velocities at high hydrostatic pressures, piezoelectric properties of some rocks as well as magnetic and thermal properties, are described. The review shows examples of application of the neutronography data along with other physical and petrophysical methods used to resolve fundamental problems in geology and in geophysics, such as reconstruction of the deformations and strains in the lithosphere and studies of the metamorphic, geodynamic and evolutionary processes addressed to data on structures of the deep-seated samples (xenoliths, amphibolites and gneiss taken from superdeep boreholes). Results of investigation of abnormal properties of some rocks which appear at a high temperature and pressure and possibilities of their application for the physics of destruction and for development of the earthquake models are discussed.

Introduction

The neutrons came into use in different spheres of natural sciences as well as in the Earth sciences shortly after they were discovered.

Differences of minerals and rocks as regards the γ -ray properties, activation characteristics of their nuclei and peculiar features of interaction with the neutron radiation, make a physical basis of the nuclear geophysics methods and serve as a prerequisite for creation of new methods for investigation of a composition of the geological materials and the

mining and geological objects [*Nuclear geophysics*, 1961].

In 1936 Hevesi and Levi proposed a nuclear physics method for determining the substance composition, that was based on activation of the atomic nuclei and on investigation of the radioactive radiation occurring due to a variation of the nucleonic composition or of the energy state of the nuclei.

The neutron activation analysis has gained a wide acceptance in the world and it serves for identification and for a quantitative assessment of the amount of different elements in the samples of minerals, ores, soils in water and in air. The activation analysis is most effectively used in determining content of noble less-common metals and non-ferrous metals, when ores and their after-products having a complicated chemical composition are analyzed [*Activation analysis...*, 1967; *Neutron-activation analysis*, 1966; *Steinnes*, 1977; *Vaganov*, 1981].

Pontecorvo, one of the closest collaborators of Fermi in the Roman University, after his arrival to the USA, where he became a Head of the geological department, proposed

Copyright 2003 by the Russian Journal of Earth Sciences.

Paper number TJE03132.

ISSN: 1681–1208 (online)

The online version of this paper was published 18 August 2003.

URL: <http://rjes.wdcb.ru/v05/tje03132/tje03132.htm>

and introduced into practice in 1940 a new and an effective method of the oil and gas prospecting – a neutron logging [Pontecorvo, 1941].

At the present time, geological services in many countries make a wide use of different modifications of the neutron logging: a neutron γ -ray logging, a neutron-neutron logging, a neutron logging on thermal and fast neutrons, a pulsed neutron logging.

The neutron logging based on the neutron-flux density measurements in a well even now is used for the geophysical investigation of the exploratory and production wells, for distinguishing the ore seams and for finding out their content of the neutron strong absorbing elements, for a lithologic separation and correlation of sections [Flerov, 1960].

Studies of different types of the neutron scattering in the condensed matter aimed at investigation of their structure are given a general term – neutronography [Nozik *et al.*, 1979; Ozerov, 1997]. Problems that are solved with the use of the neutronography are similar in many respects to those that are solved with the help of a well developed and a more readily X-ray diffraction. The use of neutrons, however, brings radically new possibilities, that are quite unique at times and that are beyond the rich of the X-ray beams.

Fundamental advantages of the neutron methods, that are based on the phenomenal properties of the neutron allow to extend the number of problems to be resolved in the condensed matter physics.

Length of the thermal neutron wave corresponds to typical interatomic distances in solid bodies. This feature of the thermal neutrons makes it possible to investigate the structure and texture of solid bodies, minerals and the mineral associations and their variations due to an external influence.

Progress in the structural and magnetic neutron diffraction, in the neutron spectroscopy and reflectometry are well known. Application of the scattering neutrons helped to resolve many fundamental and applied problems in the physics of the condensed matter in chemistry, biology, medicine and in the materials science and in the Earth sciences [Aksenov, 2000].

A new approach to the neutron diffraction texture analysis that is used along with some other physical methods for investigation of the geological properties of materials for the purpose of resolving fundamental problems in geology and geophysics has appeared in the last decade [Sobolev and Nikitin, 2001].

This review covers major achievements in the Earth sciences that were attained with the use of the neutron diffraction analysis.

I. Textures of Geological Materials and the Neutron Diffraction Texture Analysis

1.1. Crystallographic Textures and Shape of Rocks

A term “texture” is widely used in geology. The same term can be met in the metalphysics and in the material science. As to geologists, they traditionally understand

that textures mean a wide class of terrestrial formations, for example, geological objects of different scale ordered in a different way and ordered heterogeneities, that have certain elements of symmetry. According to the scale, different ranks of texture are distinguished, which differ in the spatial characteristics and in the time of formation. Thus, layers of a concentrically anisotropic structure of the Earth’s crust are the most large-scale textural elements of lithosphere. These form a sedimentary-volcanogenic, granite-metamorphic and other layers. Alternation of strata textures (made up of packets, layers) connected with alternation of rocks of different genesis are well represented in the crystalline masses. The systems of small fractures, hierarchy of parallel cracks, columnar structures like the basalt organs etc. are less frequently occur.

Two major types of textures can be distinguished in the minerals forming the rocks. These are a crystallographic texture and a mechanical texture (or the shape texture).

Crystallographic texture. The crystallographic texture means a preferred orientation of the crystal lattice of monocrystals (grains) that form a polycrystalline material. The rocks represent single-phase or multiphase polycrystalline aggregates, whose preferred grain orientation is formed during crystallization, plastic deformation, recrystallization, creep, β – α transitions, sedimentation etc. [Skrotzki, 1994].

Crystallization. The grains growing in the material during crystallization of the substance in the melt or in the solution acquire a preferred orientation. Type of the texture, which is formed during crystallization is governed by the geometric and crystallographic selection laws. The crystallographic selection brings the polycrystal to a state with a minimal internal energy as a result of a preferred growth in a direction of the crystallographic axes with the most dense packing of atoms. When the geometric selection is employed, origination of the texture formation is controlled by a preferred orientation of nuclei in the substratum and a crystallographic direction with the maximum growth rate.

Deformation. In case of a plastic deformation of the polycrystalline materials, preferred orientation of crystallites [Skrotzki, 1994; Wenk, 1985] takes place due to an intercrystalline dislocation gliding [Honicomb, 1972; Sachs, 1928; Taylor, 1938]. Thus, for example, while the deformation is going on with only one slip system taking part, a single monocrystal reorients into position when glide plane is perpendicular to the direction of the maximum compression and the glide is parallel to the direction of extension. If a polycrystal having a chaotic orientation of grains is deformed by gliding inside each grain so that no breaks occur at the boundaries, then the change of shape of any grain must agree with the change of shape of the neighbouring grains and with the shape of the entire body as a whole. If the grain possesses five independent slip systems, this grain may suffer a general modification of the shape during the glide. All grains must follow this condition (Mises condition) so that the polycrystal would be capable of withstanding great plastic variations of the shape. When deformation of the polycrystal is taking place by way of gliding the individual grains become constrained by their neighbours and

various rotations of the crystalline lattices are taking place in these grains. A relative role of rotation of the lattice may be assessed, if to assume that each grain of the polycrystal undergoes a similar low deformation so that deformation of the whole body is uniform. The rotational component of the plastic deformation of each grain dictates physically appearance of a portion of grains (greater or smaller portion) of the volume of the polycrystal having close orientations.

Recrystallization. Recrystallization as a physical process causing modifications of the structure and texture of rocks at different evolution stages can be assigned to a various metamorphic reactions. Formation and modification of the recrystallization textures takes place when the deformed geomaterial is heated or cooled down (or during deformation) and caused by replacement of the initial grains with a distorted lattice by new ones having a more developed structure. It should be noted that the mineral composition may change sometimes, while structure must remain unchanged or, vice versa, with the unchanged mineral composition the size, shape and orientation of crystallites change. Primary, cumulative, secondary and dynamic recrystallization are recognized [Kocks *et al.*, 1998; Wasserman and Greven, 1969; Wenk, 1985].

A combination of acting recrystallization mechanisms depends upon a great number of parameters, including pressure, temperature, strain rate, deformation path, grain size and a fluid content. A properly established recrystallization mechanism based on the investigation of the structure and texture of the deformed rock is an essential part of the deformation history [White, 1977].

Shape texture. The shape texture is interpreted as the oriented component parts with an anisotropic outer shape. Mechanical textures in metals, for example, are formed by crystallites having an extended or a fibrous shape [Nikitin, 2000; Wasserman and Greven, 1969]. The shape texture the rocks is created by parallel layers, streakiness of the mineral associations, oriented cracking and microcracking, grains of extended shape, flat and acicular defects, oriented intergranular boundaries [Kocks *et al.*, 1998; *Tectonophysics...*, 1971; Volarovich, 1972]. The value of the rock anisotropy properties depends on concentration and configuration of pores. With all variety of the rocks the main are two types of pores [Volarovich *et al.*, 1974]:

- volumetric pores – their sizes are the same in all directions;
- slit-like pores (as well as microcracks) – size in one direction is several orders greater than in other directions.

The experimental observations have shown existence of the ordered systems of spheroidal and needle-shaped microcracks in the rock samples [Hadley, 1976; Kranz, 1983].

Formation of the oriented crack hierarchies in the rocks at different scale levels has been studied in detail and it has general patterns that are accounted for by the existent theories of crack formation. The crack systems observed in nature are complicated and varied. When the samples are tested for compression either tensile cracks (surfaces are parallel to the compression axis) or shear cracks at an angle to the compression axis appear. In the first case behavior of the rock corresponds more to a simple compression, while in

the second case it corresponds to a triaxial compression at a low hydrostatic pressure.

The Griffith theory [Griffith, 1924] is one of the early crack formation theories. Today the mechanics and physics of rock fracture has quite a powerful instrument which was developed by A. N. Stavrogin [Stavrogin, 1969], L. M. Kachanov [Kachanov, 1961], S. N. Zhurkov [Zhurkov, 1968], E. I. Shemyakin [Shemyakin, 1999], G. I. Barenblatt [Barenblatt *et al.*, 1966], G. P. Cherepanov [Cherepanov, 1967], J. R. Rais [1982] and by others. Any material in reality has cracks which vary in size, form and orientation. It means that tensile stresses are developed at the ends of some cracks even at a simple compression. The growth of favorably oriented cracks and their preferred orientation are due to such (induced) tensile stresses. There is evidence that at a simple compression cracks grow along the curved surfaces until they become parallel to the compression axis.

Different pattern of preferred orientation in the continental crust confirm that one of the most important types of mechanical behavior, which appeared in the rock, in the folded zones connected especially, is a flow in a solid state. Some of these textures observed in nature are similar to textures obtained during experiment. The rocks are to capable to the conneced flow, evidently, at any combination of physical conditions which occur in lithosphere.

A more sophisticated models, which describe shape textures were appeared along with development of a theory of elasticity of microheterogenous anisotropic media, based on a random field theory. The author [Salganik, 1973] has analyzed a problem related to determination of effective characteristics of a body with the shape texture, which considers influence of a stress strain upon development of cracks. This was done theoretically in the frames of mechanics of a heterogenous continuum. More attention was concentrated in another work for statement and general analysis of the kinetic equation for the distribution function of variables, that specify form, location and orientation of the cracks in the configurational space [Petrov *et al.*, 1970]. The problem related to connection of a random distributed cracks with effective parameters of the elastic medium was analyzed in the work mentioned here [Chekin, 1970].

Having used the approach of Eshelby as the basis for solving the problem of a solitary ellipsoid inclusion in an infinite matrix and a generalized singular approximation (GSA), authors [Kalinin and Bayuk, 1994] made a proposal to solve the problem of determination an elastic anisotropy of the medium with the oriented penetrated cracks of an arbitrary form and concentration. An isotropic matrix penetrated by a system of the oriented cracks as hollow ellipsoids, was the model of the medium.

However, a model of origination of the shape texture in the quartz-bearing rock was proposed even earlier [Nikitin and Arkhipov, 1992]. First of all, influence of a thermally initiated polymorphic transformation on the process of transition of the medium from the isotropic state into the anisotropic one was considered in this model; secondly, a coexistence of three components of quartz with different anomalous properties in the material was admitted in the model. It was shown that a microstructure ellipsoidal elements oriented in parallel to large axes, thus transferring

the rock into an anisotropic state, appear in the microplasticity zones, formed due to a $\beta - \alpha$ transition under of non-equiaxial mechanical stresses. A tensor of the rock elastic characteristics was also calculated.

There is a clear concept in geophysics now that the crystallographic texture and shape texture are central factors that control anisotropy of rocks [Aleksandrov and Prodaivoda, 2000; Bayuk *et al.*, 1982; Babuska and Cara, 1991; Karato, 1987; Kocks *et al.*, 1998].

The less symmetry of crystals forming the rock is and the more contrast their own anisotropy is the greater becomes influence of the crystallographic texture on anisotropy of the physical properties. The elastic properties of materials (elastic constants first of all) and magnetic properties of ferromagnetics are mainly controlled by the texture. The textures of materials, which are formed by crystallites having a non-cubic lattice, cause the anisotropy of heat conductivity, thermal expansion, electric conductivity and other characteristics.

1.2. Investigation of Rocks by Optical Methods, Electron and X-ray Diffractions

Optic method for measuring the preferred orientation of grains in the rock. As early as at the beginning of the twentieth century the optic methods for investigation of the preferred orientation of minerals in the rock were started to use. These are widely employed even now in the field laboratories, in the geological expeditions and in the universities to determine the crystallographic texture of rock samples and give some other supplementary information on the sample mineralogy.

The fact that the useful information is limited to data about orientation of the optic axes of the grains arranged on the thin section only is the major disadvantage of the optic methods. The maximum shine method, the universal stage method and the photometric method are the main optic methods used for determination of preferred orientation.

Maximum shine method. The maximum shine method is based on a different speed of etching of various crystallographic planes. Orientation of individual grains of the polycrystalline rock is judged by way of analyzing angles of reflection of the light beam by the known faces revealed by etching $[hkl]$ or the form and arrangement of the etching pits with the help of an electron microscope or an optic goniometer.

Photometric method. The photometric method is based on interference of the polarized light beams passing through a crystal. The interference colors of a crystal change if it is rotated with respect relative to a polarizer and analyzer of the polarized microscope.

The intensity profile depending on orientation of the thin section is calculated for a set of grains, which is then compared with a profile obtained by a photometer. These profiles are decomposed into a certain number of profiles, each of them corresponding to a c-axis orientation. These orientations may be represented on the pole figures. This method

which was proposed by *G. P. Price* [1973], belongs to integrated methods as it does not present a relation of the c-axis orientation with orientation of single grain.

The computer-integrated polarization microscopy combines the Price method with image processing [Heilbronner and Pauli, 1993]. When viewing the thin section through crossed polarizers and inserted gypsum lambda plate, it is possible to observe the change of interference color (orientation image). Different grains have different color depending on properties of a double refraction of the mineral, orientation of the c-axis and on thickness of the section. For example, on the thin section 20–30 μm thick in thick quartz grains taking into account its rather weak double refraction will display different shades of blue, yellow and the 1st order red.

If polarizers are N-S and W-E oriented, then the quartz grain with the c-axis parallel to the north-south direction (azimuth $\varphi = 0^\circ$, inclination $\vartheta = 0^\circ$) displays red color of the 1st order. During clockwise rotation the interference colors change: $\varphi = 45^\circ$ – blue, $\varphi = 90^\circ$ – red, $\varphi = 135^\circ$ – yellow, $\varphi = 180^\circ$ – red. During the complete revolution this sequence repeated twice. The increase of inclination angle and shifts of the c-axis reduce the color contrast the blue and yellow towards the red color of the 1st order up to an extreme case, when the c-axis becomes perpendicular to a plane of the thin part of the section (at $\vartheta = 90^\circ$ the grain shows the red color irrespective of angle φ).

If the c-axis of the quartz grain is aligned on all the possible directions, then having recorded the observed interference colors on an equal area projection, we obtain an interference color stereogram (ICS). Let us note that this stereogram can be obtained by calculation from the interference spectrum for each position of (φ, ϑ) on a stereographic net. The ICS can be considered as the color maps, which correlate the specific colors with orientation of the c-axes.

Due to a symmetry of the quartz crystal, however, relation between color and orientation is not unambiguous. Usually in practice the microscope stage is rotated to obtain supplementary information about orientation of the grain. A sequence of colors should be established for any given initial position. Further, the rotation required for coincidence with the red color of the 1st order, fixes the azimuth φ , and the color contrast intensity between the yellow and blue zones determines the angle of inclination ϑ . The problem of definition the signs is resolved by inclining the section relative to the microscope stage. Thus, orientation of the c-axis is defined unambiguously.

Universal stage method. The described above methods of investigation of the optical properties of crystals are developed applicable to the polarizing microscope with a stage rotating around one axis i.e. the microscope axis.

E. S. Fedorov developed a new method in principle at the end of the XIX century and he named it as U-stage or theodolite method [Fedorov, 1893]. Analysis of crystals by this method is done on a special (Fedorov) stage, which is fixed on a conventional stage of the polarizing microscope. The Fedorov stage has several axes allowing to take the object under investigation from a position perpendicular to the microscope axis and to rotate it in different space directions.

Measurement of the rock grains orientations on the

U-stage is based on the anisotropic optic properties of crystals. The properties depend on crystal symmetry and may be described by the optic indicatrix with its principal axes $n_\alpha, n_\beta, n_\gamma$.

In the case crystals of trigonal, tetragonal and hexagonal crystal symmetry one optical axis exists and coincides with the main symmetry axes of crystal. In the uniaxial minerals (quartz, calcite) the c-axis is the single "optical" direction which can be measured. Two or more crystallographic directions must be determined in addition to the c-axis to obtain a complete orientation. The optical method is not helpful for the purpose in the case of quartz.

Triclinic, monoclinic and orthorhombic minerals possess two optic axes. Orientation of the optic indicatrix relative to the crystallographic axes is more complicated than in the uniaxial case. It depends on the symmetry of the crystal and on a chemical composition of the mineral. In orthorhombic minerals (olivine, for example), the optic indicatrix axes are parallel to the main crystallographic directions, and, hence, a complete orientation can be determined directly from the measurements of indicatrix.

In monoclinic minerals (hornblende) the indicatrix axis deviates from the crystallographic c-axis by different angles depending upon the composition of the mineral under investigation. Therefore, a supplementary information is required for an unambiguous definition of the orientation of crystal. For triclinic minerals like plagioclase, none of the main crystallographic directions can be defined directly from the indicatrix. Its relative positions change in dependence on the mineral composition [Benn and Mainprice, 1989; Kruhl, 1987]. Therefore, to determine a complete orientation of the low-symmetric minerals orientation of at least one crystallographic plane must be measured in addition to the indicatrix axes.

A procedure for determining the preferred orientation of minerals in the rock samples was developed by B. Sander [Sander, 1923].

Electron diffraction. The use of the scanning electron microscope (SEM) for determination of the preferred orientation of grains is a rather new method and, therefore, it is not very widespread. The electronic channeling (EC) and the electronic backscattering diffraction (EBSD) methods are distinguished. Fundamentals of the SEM method are described in detail in the work of [Holt *et al.*, 1974].

As a result of the electronic channeling unique configuration of lines and bands, which characterize orientation of the crystallite at the point of beam incidence, is obtained. The EC technique [Lloyd, 1994] is based on the fact that a small portion of backscattered electrons originated from the "channeling" of incident electrons between the lattice planes. To maximize the emission signal due to a particular set of atomic planes, the angle of incidence between the electronic beam and the planes must change by at 2θ during the scanning process. Moreover, the beam must be collimated because changes in emission can be observed only when a great part of electrons move in the same direction. The EC image recorded by electron microscope is a point diffraction pattern, which can be considered as a practically non-distorted projection of a reciprocal lattice plane.

Electronic back-scattering Kikuchi patterns create a geometrically equivalent images. EBSD form when a stationary beam strikes an inclined sample so that the incident beam has relatively low angles of incidence ($\sim 10\text{--}30^\circ$). An optimum spatial resolution of the EBSD method is $0.1\text{--}1.5\ \mu\text{m}$ that is better than for the EC method ($1\text{--}10\ \mu\text{m}$). However, the sample is inclined and this causes anisotropy of resolution. The angular range of EBSD is $\sim 40\text{--}80^\circ$, unlike the EC $\sim 20\text{--}25^\circ$. The large range of EBSD helps to index the reflexes.

Analysis of the EC pattern is based on comparison of a pattern obtained on a sample with the so-called "ECP maps" (electronic challenging pattern) made up of individual EC events. These maps contain the mineral lines pattern and can be represented on a spherical surface or as on to projection on to plane. In order to determine the mineral grain orientation the sample picture, which is a small section of the whole pattern brought into unequivocal coincidence with the pattern on the ECP map. The lines are indexed and orientation of the grain relative to the coordinate system of the sample is found with the help of necessary rotations. The patterns can be compared visually, but computer-aided indexing and plotting of fabric diagrams for each crystallographic direction is done in practice [Schmidt and Olesen, 1989].

An orientation imaging microscopy method (OIM) [Adams *et al.*, 1993] is an automated analysis of the electronic backscattering pattern for orientation measurements. The sample is fixed on the microscope stage for a two-dimensional positioning. The EBS pattern is observed on the screen with the a high-resolution camera-recorder, fixed by computer and orientation of the crystal is determined automatically. While the sample is analyzed the stage is shifted to a new position and pattern of another grain is recorded. Thus, the sample surface is scanned on a regular grid with the selected step size. A practicable rate is about 3000 measurements per hour thus allowing to obtain statistically reliable data in a short period of time. To date the ORM method is restricted by monophase materials. The use of this method might be connected with resolving also specific problems related to local investigations such as determination of the recrystallization nuclei orientation etc.

X-ray method. Measurement of the pole figures with the X-rays is based on diffraction when radiation of given range is scattered on the atoms of crystalline lattice. The scattering originates from induced oscillations of the atom electrons under the influence of the electromagnetic field of the X-ray incident wave. The X-ray diffraction is widely applied to crystals because the order of the interatomic distances in a crystal is the same as order of the X-ray wave length. Two waves reflected from the similar lattice planes with the distance d_{hkl} is characterized by a path difference Δ . If $\Delta \neq n\lambda$ (λ - the radiation wavelength, n - the integer value), then the interfering waves completely delete each other.

Intensity is observed only if $\Delta = n\lambda$. Connection between λ , d_{hkl} and angle θ , between the incident beam and the reflecting lattice can be determined from purely geometrical relationship (Bragg's law). By keeping λ constant and

changing θ , it is possible to record a complete X-ray diffraction pattern, if the crystal is in a reflecting position for all lattice planes.

The X-ray experiment is done in the following way. The sample is placed in the center of circle of the goniometer circle. The incident beam falls on the sample at an angle θ , the reflected beam can be seen at an angle 2θ with respect to the primary beam. This condition is fulfilled, if the focusing circle intersects the goniometer circle at the collimator and receiving slit position and contacts the sample surface as well. The dispersion vector corresponds to a normal to the lattice plane (hkl), which is in a reflecting position.

During measurement of pole figures the θ is set to the correct value of the desired Bragg reflection (hkl) and remains constant. The spatial orientation of the sample is changed systematically and the intensity I_r of the reflected beam is measured for each position. The reflected intensity is proportional to the scattering volume part of the volume V_{hkl} , if the size of grains in the sample is not uniform, it is also proportional to a number of the reflecting crystallites N_{hkl} .

Sample positioning is made with the help of the Euler cradle by rotating the sample about two perpendicular axes. Two X-ray experiment conditions are recognized:

- 1) back reflection mode (the scattered beam is observed at the same side of the sample);
- 2) transmission mode (the scattered beam passes through the sample).

Advantages and disadvantages of indicated X-ray experimental mode are as follows. The texture of the polycrystalline material is a statistical ensemble of crystallites, so to obtain a meaningful mode a statistically representative number of crystallites or grains is required. It is necessary to have 10^4 up to 10^5 grains to get reproducible pole figures. The known properties of the X-rays, namely a strong absorption by the material and a small diameter of the beam limits their use for small and thin samples and for the fine-grained material with the grain size below 10–20 μm . These limitations of the method permit to investigate the sample surface only as the X-rays penetrate the sample just from few to several micrometers. The X-rays measure the local texture on the sample surface. It is possible to get only incomplete pole figures because of the high orientation dependent absorption and limitations by defocusing (broadening of peaks due to different cross sections of the reflected beam) of the Bragg reflection, when a flat sample is inclined. This disadvantage might be overcome partially by a precise scanning equipment, e.g. a combination of measurements in transmission and reflection geometry as well as sophisticated data analysis. Usually the X-ray diffraction is limited to monomineral rocks of orthorhombic or higher crystal symmetry.

A comparative analysis of texture measurements of the carbonate rock samples, performed by the X-ray and the neutron diffraction methods, was made in the work by [Wenk *et al.*, 1984]. The authors [Ullemeyer *et al.*, 2000] made a comparison of texture determination of two-phase muscovite-quartzite sample with four different methods used in the geological sciences: optical U-stage, electron backscattering diffraction, X-ray back reflection texture goniometry and time-of-flight neutron diffraction. The work discusses advan-

tages and disadvantages of these methods in investigation of geological materials.

1.3. Measurement of Pole Figures by Neutron Diffraction. Main Advantages of the Neutron Diffraction Texture Analysis

The major task of the texture analysis lies in obtaining information about the distribution of crystallite orientations in the sample under investigation. Preferred orientations are visually represented by pole figures. A graphic representation of the distribution function P_{hkl} of normal poles to one specific crystallographic plane (hkl) is also often referred to as a pole figures. The function P_{hkl} proper is called the pole figure. Stereographic projection is usually used for graphic representation of the function. The function P_{hkl} is the probability of coinciding the normal to (hkl) plane with different directions in the sample.

The normal to the (hkl) plane in respect to the sample coordinate system is specified by the polar angle Φ and azimuth γ , where $\gamma = (\Phi - \pi)$. Thus, the distribution function P_{hkl} is represented as $P_{hkl}(\Phi, \gamma)$. Any function which depends on the direction can be expanded in a series in spherical functions k_l^μ . The function P_{hkl} is expanded in the symmetric spherical functions k_l^μ with the symmetry of the sample. $P_{hkl}(\Phi, \gamma)$ is presented as

$$P_{hkl}(\Phi, \gamma) = \sum_{l=0}^{\infty} \sum_{v=1}^{N(l)} F_l^v(hkl) \dot{k}_l^v(\Phi, \gamma). \quad (1)$$

In practice the infinite series (1) is replaced by a finite sum, breaking at a certain $l = l_{\text{max}}$. The expansion coefficients are expressed in terms of the experimentally pole figure as

$$F_l^v(hkl) = \int_0^\pi \int_0^{2\pi} P_{hkl}(\Phi, \gamma) \dot{k}_l^v(\Phi, \gamma) \sin \Phi d\Phi d\gamma. \quad (2)$$

Measurements of pole figures are by neutron diffraction are carried out on sphere or more frequently on cubic samples. While texture samples with polished surfaces or thin sections are necessary for X-ray diffraction, no special preparation for neutron measurements is needed. Furthermore, neutron diffraction allows to measure complete pole figures.

Modern texture diffractometer equipped with the position-sensitive or multidetector system [Schäfer, 2002] permits to measure several pole figures simultaneously. Moreover, the special profile analysis is applied to separation of overlapping Bragg reflections on the spectra [Ullemeyer *et al.*, 2000].

The textured polycrystal sample, practically at its any position with respect to the neutron beam, has groups of crystallites arranged in the way that the Bragg condition is fulfilled. In order to determine the orientational dependence of the intensity of the given reflex (hkl), it is necessary to rotate the sample with respect to the incident beam. A

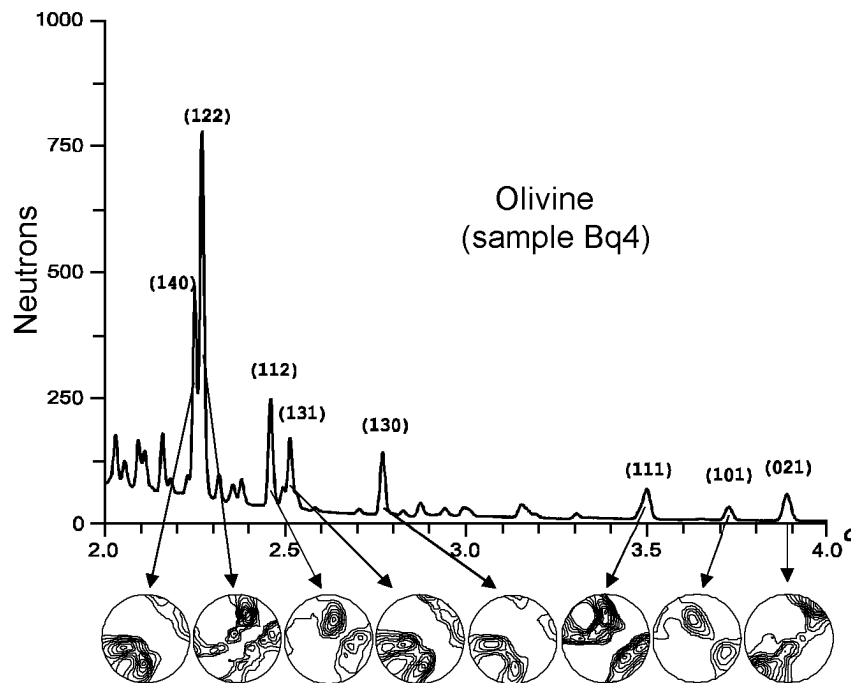


Figure 1. Diffraction spectrum and pole figures corresponding to some indexed Bragg reflections.

special texture goniometer is used for this purpose. An individual diffraction spectrum corresponds to each sample position. Determining the integral intensity of one reflex from this spectrum we obtain a value of the pole density for one point corresponding to angles Θ and φ on the pole figure. Because one can calculate the pole densities at the same point for different pole figures determining intergrated intensities of these Bragg reflections (Figure 1).

The pole figures are indexed after the reflexes caused by the scattering of a given wave length from the crystallographic planes with same parameter of the lattice d (Figure 1). Theoretical spectra, calculated with the structure parameters of crystals by Bragg diffraction law, are used for indexing the spectral maxima. To find the pole density the integral intensity of reflexes with identical indices (each diffraction peak is approximated by a normal distribution) is to be determined. For calculation of the pole density background values are determined over reflex interval. Corrections to be reflectivity of the interplanar spacing sensitivity of detectors etc are introduced. As a result, figures form the data arrays the pole densities and may be visualized on a stereographic projection.

The main advantages of neutron scattering application for texture analysis of geological material:

- (1) high statistical representation (thousands of grains compared with hundreds of grains, measured by optic microscope);
- (2) investigation of volume textures rather than local (surface) textures by X-ray diffraction;
- (3) study of both coarse-grained and fine-grained natural materials;
- (4) texture analysis of low-symmetry minerals;

(5) investigation of multiphase rocks, permitting a texture analysis of individual mineral components, that is not possible for other diffraction methods and for direct methods of the texture analysis;

(6) investigation of the texture evolution of samples placed in chambers at the high pressure and temperature, that is not possible both for other diffraction methods and for direct methods of the texture analysis.

The quantitative texture analysis using neutrons is applied now to monomineral and multiphase geological materials [Chateigner *et al.*, 1999; Lobanov *et al.*, 2002]. The application of a new Riveld technique combined to ODF calculation will be method of choice in polycrystalline diffraction-data evaluation. The main targets are to obtain the orientation distribution in the case of low-symmetry compounds and to analysis the crystal structure in the presence of strong texture.

Several attempts were made to combine structure, texture and stress/strain analysis using neutron diffraction. R.-H. Wenk [Wenk *et al.*, 1994] proposed a method using the whole diffraction spectrum rather than extracted peak intensities by combining the quantitative texture analysis with the Rietveld crystallographic method. The feasibility of the Riveld texture analysis are demonstrated with neutron time-of-flight data of experimentally deformed calcite [Lutterotti *et al.*, 1997]. It was possible to obtain a quantitative information on texture, crystal structure, microstructure and residual stresses on the basis of incomplete pole figures and from regions of the diffraction spectrum containing the overlapping peaks. Neutron diffraction has the potential to investigate evolution of microstructures, including the dehydration, phase transition, structural changes in the

minerals as well as stresses/strain using experimental and measuring complexes such as SKAT-CUC and EPSILON-MSD (Dubna, Russia) or HIPPO (Los Alamos, USA).

1.4. Quantitative Texture Analysis

Mathematically the crystallographic texture is described in terms of the orientation distribution function (ODF) [Bunge, 1982; Matthies, 1979; Matthies et al., 1988; Viglin, 1960]. However, ODF cannot be obtained directly from the experiment. It is possible to measure only its integral projections, pole figures (PF), which represent intensities of the diffraction reflections from certain crystallographic planes of crystallites. The main task of the quantitative texture analysis is the ODF computation from a finite number of experimental number of PFs. Methods of Roe-Bunge [Bunge, 1965; Roe, 1965] and the ODF approximations by standard functions [Bukharova and Savelova, 1993; Nikolaev et al., 1992; Savelova, 1984; Savelova and Bukharova, 1996] are most widely employed to resolve this task.

The relative orientation of crystallographic axes of crystallites in the polycrystalline material can be determined by rotation of g . If to assume that the orthogonal coordinate system K_A (laboratory coordinate system) is connected with the sample under investigation and the orthogonal coordinate system K_B^i (crystallite coordinate system) is connected with the crystalline lattice of the i -th crystallite, then orientation of g defines the rotation that transforms the coordinate system K_A into K_B^i . This rotation is set by three Euler angles $\{\varphi, \vartheta, \psi\}$ and belongs to a rotation group of a three-dimensional Euclidean space $SO(3)$.

The ODF $f(g)$ defines a volumetric part of crystallites of the material whose crystallographic coordinate system is turned with regard to the laboratory system through angles φ', ϑ' and ψ' , lying inside a solid angle dg , which represents an invariant measure on group $SO(3)$:

$$\frac{dV(g)}{V} = f(g)dg = \frac{1}{8\pi^2} f(\varphi, \vartheta, \psi) \sin \vartheta d\varphi d\vartheta d\psi. \quad (3)$$

The integral of this function on a certain domain u is interpreted as a probability to find a random orientation g in this domain.

If a certain crystallographic plane with the normal is selected in the system then the PF $P_{\vec{h}_i}(\vec{y})$ determines a volumetric part of crystallites, for which different directions \vec{y} of the coordinate system K_A are in the infinitesimal volume with the normal \vec{h}_i directions to the i -th crystallographic plane of crystallite. Let us note that directions \vec{y} and $-\vec{y}$, as well as directions \vec{h}_i and $-\vec{h}_i$, are indistinguishable physically in the experiment and, consequently, the relevant PF become indistinguishable. Then probability that volume v of the randomly oriented crystallites in the sample will have a direction \vec{h}_i is

$$p(v) = \int_v P_i(\vec{y}) d\vec{y} = \frac{1}{4\pi} \int_v P_i(\varphi, \vartheta) \sin \vartheta d\varphi d\vartheta. \quad (4)$$

Here, φ and ϑ – spherical coordinates of the vector \vec{y} . The ODF $f(g)$ and PF $P_i(\vec{y})$ are bound together by an integral relation:

$$P_{\vec{h}_i}(\vec{y}) = \frac{1}{4\pi} \int_0^{2\pi} \{f([\vec{h}_i, \xi]^{-1}[\vec{y}, 0]) + f([-\vec{h}_i, \xi]^{-1}[\vec{y}, 0])\} d\xi, \quad (5)$$

where $[\vec{y}, 0] = \{\varphi, \vartheta, 0\}$ – rotation in $SO(3)$, $[\vec{h}_i, \xi]^{-1}$ – rotation reverse to $[\vec{h}_i, \xi]$.

Thus, solution of the task of restoration of ODF from PF mathematically is in finding $f(g)$, satisfying the system of the integral equations (3), from the finite set obtained from the PF experiment $P_{\vec{h}_i}(\vec{y})$.

A method for calculation of ODF proposed in the work of [Bunge, 1965; Roe, 1965] has received a wide recognition. This method consists in presentation of ODF as a series of generalized spherical harmonics and the pole figures as a series of spherical harmonics. In this case for ODF $f(g)$, the following expansion in series of generalized spherical harmonics $T_{mn}^l(g)$ is right:

$$f(g) = \sum_{l=0}^{\infty} \sum_{m=-l}^l \sum_{n=-l}^l C_{mn}^l T_{mn}^l(g), \quad (6)$$

where coefficients of the ODF expansion in series are found in the following way

$$C_{mn}^l = (2l+1) \int_{SO(3)} f(g) \bar{T}_{mn}^l(g) dg. \quad (7)$$

Here and further the complex-conjugate functions are marked with a bar.

The PF can be presented as an expansion in series of spherical harmonics $Y_l^m(\vec{y})$:

$$P_{\vec{h}_i}(\vec{y}) = \sum_{l=0}^{\infty} \sum_{m=-l}^l F_m^l(\vec{h}_i) Y_l^m(\vec{y}), \quad (8)$$

where $F_m^l(\vec{h}_i)$ – expansion coefficients. The integral relation (5) and expansion in series (6) give the following formula, which expresses the PF through the ODF expansion coefficients C_{mn}^l :

$$P_{\vec{h}_i}(\vec{y}) = \sum_{l=0}^{\infty} \sum_{m=-l}^l \sum_{n=-l}^l \frac{4\pi}{2l+1} [1 + (-1)^l] C_{mn}^l \bar{Y}_l^n(\vec{h}_i) Y_l^m(\vec{y}). \quad (9)$$

Relations (8) and (9) in the Roe-Bunge method are considered systems of the algebraic equations for the unknown C_{mn}^l , which are usually found by the least-squares method. A priori information about symmetry of the crystallite and the sample (number of unknowns reduces) and about sharpness of the texture (preliminary information about the expansion length (6) of truncated series) is used for an unambiguous determination of these coefficients.

Let us note, that it follows from the relation (9) that the pole figures do not depend on the odd component of ODF.

Therefore, knowledge even all theoretically possible PF can present information only about the expansion coefficients of the even component of the ODF. Thus, the ODF cannot be determined unambiguously, in principle, from PFs [Matthies, 1979].

A number of methods has been developed recently, which with some additional assumptions about the ODF, permit to find a unique solution to the ODF reconstruction problem from PFs by introducing a priori constrains about the ODF structure. The ODF approximation by normal distribution on group belongs to these methods. In this case, the ODF might be presented as a linear combination of normal distribution on group $SO(3)$

$$f(g) = \sum_{k=1}^N A_k \Phi_k(g, g_{0k}, \varepsilon_k), \quad (10)$$

where A_k – positive coefficients (weight), $\Phi_k(g, g_{0k}, \varepsilon_k)$ – normal distribution with maxima at the point g_{0k}, ε_k – scattering parameters (analogs of dispersion). These parameters are found using the comparison of the theoretical PFs from ODF of form (8) with the experimental PFs, for example, with the help the least-squares method.

One of the first proposed approximations of ODF with a normal distribution is in the work of [Bunge, 1982]. This distribution was obtained by analogy with the known Gaussian distribution on a straight line.

However, ODF construction on the basis of a central limit theorem of the probability theory of is a more rigorous approach. This approach exactly was employed in the work by [Savelova, 1984; Savelova and Bukharova, 1996], where circular and non-circular normal distribution, so-called central normal distribution, is analyzed. The central normal distribution is given by:

$$\begin{aligned} \Phi(g, g_0, \varepsilon) &= \\ &= \sum_{l=0}^{\infty} (2l+1) \exp(-l(l+1)\varepsilon^2) \frac{\sin((l+1/2)t)}{\sin(t/2)}, \end{aligned} \quad (11)$$

where $\cos t = (Tr(g_0^{-1}g) - 1)/2$.

The PF responding to this distribution are written as

$$\begin{aligned} P_{\vec{h}_i}(\vec{y}) &= \\ &= \sum_{k=0}^{\infty} (4k+1) \exp(-2k(2k+1)\varepsilon^2) P_{2k}(\cos \vartheta), \end{aligned} \quad (12)$$

where $P_{2k}(\cos \vartheta)$ – normalized Legendre polynomials, and $\cos \vartheta = (\vec{h}_i \cdot g_0 \vec{y})$. Functions (11) and (12) can be approximated by more simple expressions:

$$\begin{aligned} \Phi(g, g_0, \varepsilon) &\approx \\ &\approx \left[\frac{1}{\varepsilon^3} \exp(\varepsilon^2/4) \operatorname{erfc}(\varepsilon/2) + \frac{1}{\varepsilon^2} \right] \frac{t/2}{\sin(t/2)} \exp(-t^2/4\varepsilon^2) \end{aligned} \quad (13)$$

for ODF and

$$\begin{aligned} P_{\vec{h}_i}(\vec{y}) &\approx \\ &\approx \frac{1}{2\varepsilon^2} [\exp(-\vartheta^2/4\varepsilon^2) + \exp(-(\pi - \vartheta)^2/4\varepsilon^2)] \end{aligned} \quad (14)$$

for PF. Representations (11) and (12) were used in the work by [Bukharova and Savelova, 1993; Helming, 1993; Nikolaev et al., 1992] for polycrystalline materials of different symmetry.

A component method [Helming and Eschner, 1990], which is applicable to crystals of any symmetry is rather frequently used for a quantitative texture analysis. It is important to note, that this method permits to make the texture analysis of two and more mineral phases simultaneously.

1.5. Neutron Spectrometers for Investigation of Textures, Stresses and Properties of Geological Materials in the World Research Centers

The neutron texture diffractometers are capable of functioning in the same way as the X-ray diffractometers on a constant wave length on stationary reactors or they may use a time-of-flight method on the pulse reactors and accelerators. The main parameters of the experimental assemblies used in different research centers for investigation of textures of the polycrystalline and the geological materials are presented in Table 1.

Diffractometers on steady-state neutron sources.

The simplest diffractometer situated at a thermal beam tube of a steady-state reactor matches a conventional four-circle diffractometer equipped with the Euler cradle as a goniometer and single-county tube, i.e. it is an instrument for investigation of structure of monocrystals. Measurements of sample-orientation-dependent intensities are made with the of a detector, positioned stationary position in the peak maximum, i.e. a step scanning is performed on an equal-area grid of the pole figure. The TEX-2 at the research reactor FRG-1 in GKSS, which is dedicated to texture analysis (predominantly of high-symmetry materials) [Brokmeier et al., 1998] belong to this type of diffractometer. In the case of the instrument with single detector, pole figures, needed for restoration of the ODF, are measured one after another, which is a time-consuming procedure.

Instruments equipped with a system of the position-sensitive detectors are very effective for the texture analysis of the geological materials. The biaxial spectrometer D1B and the powder diffractometer D20, which are functioning in the Laue-Langevin Institute (Grenoble, France), are suitable for texture measurements.

The D1B spectrometer at the high-flux source ILL in Grenoble [Wenk et al., 1986] was the first instrument for the texture investigation of the low-symmetric plagioclase. The D1B spectrometer has a system of replaceable monochromators and a movable multidetector module. The spectrometer is outfitted with a special cryostat to perform experiments over a wide temperature range.

The diffractometer D20 is characterized by a linearly bent

Table 1.

Parameters	SKAT JINR Russia	HCHP JINR Russia	GPPD ANL USA	TEX-2 GKSS Germany	HIPPO LANL USA	E3 ChRL Canada	D1B ILL France	D20 ILL France	SV7-b FZ-Jülich Germany
Size of beam, mm ²	50×50	50×30	13×51	45×45	20×20	50×50	50×20	30×50	25×40
Distance between moderator and sample, m	102.8	104.8	19.9	7.8	8.6	7.2	64.8	7.1	8.2
Distance between sample and detector, m	1	1.6	1.5	0.4–2	0.4	1.37	1.5	1.47	1
Wave length range, Å	0.8–7.6	0.8–7.6	0.2–5.7	0.8–2.7	0.2–10	0.7–4.0	1.3–2.5	0.8–2.4	0.9–2.3
Range of scattering angles, degree	90	20–170	30–150	10–120	10–150	10–120	20–140	20–170	10–90
Number of detector modules	19	7	7	1+PSD	5	PSD	PSD	PSD	PSD
Detector type	³ He	³ He	³ He	³ He	³ He	³ He	³ He/Xe	³ He	² Li
Resolution $\Delta d/d \times 10^{-3}$	≈ 7	≈ 4	≈ 7.6	≈ 8	≈ 4.5	≈ 6	≈ 6	≈ 6	≈ 13
Neutron flux on the sample, n/(cm ² s)	$\sim 10^6$	$\sim 10^6$	$\sim 10^9$	$\sim 10^5$	$\sim 10^8$	$\sim 10^9$	$\sim 10^6$	$\sim 10^7$	$\sim 10^6$

Note: PSD – position-sensitive detector.

position-sensitive detector system as well as a wide operation wavelength-range.

The texture diffractometer SV7-b mounted on the neutron beam in the experimental hall of the research reactor FRJ-2 operates in the Jülich (Germany) Research Center.

The instrument is equipped with various monochromators crystalline coatings that make possible obtaining the wave length ranging from 0.9 up to 2.3 Å. The use of special ($\lambda/2$)-filters, which suppress the higher order noise, permits to improve the experimental pole figures that are recorded during investigation of the geological materials.

The texture diffractometer is supplied with position-sensitive scintillation detector of the JULIOS-type mounted on the free-rotating platform. It is capable of covering an angle of $\Delta 2\theta = 50^\circ$. The detector has also the replacement Euler cradles that permit making measurements on the sample, both under normal conditions and under low temperatures, by placing the cradle inside a helium cryostat.

Owing to the position-sensitive detector the SV7b diffractometer is used as a working instrument for investigation of rocks mainly [Ghildiyal *et al.*, 1999; Jansen *et al.*, 1992; Will *et al.*, 1990].

Diffractometers at pulse neutron sources. The fact that the thermal neutron reactor impulse has a continuous spectrum, the thermal neutron velocity is low and there is a possibility of making the neutron energy analysis (or the wave length) in the time of flight (or TOF experiment) may be considered as the feature dictating the procedure and scheme of the diffraction experiment on the pulsed sources.

The texture diffractometer – SKAT [Ullemeyer *et al.*, 1998] functions on the IBR-2 pulsed reactor (JINR, Dubna, Russia). Its detector system, containing nineteen detectors, is arranged on a mounting ring 2 m in diameter, which is

axially symmetrical with respect to the neutron beam. The resulting time-of-flight path (distance between the moderator and detector) is 103.8 m. The detectors can be fixed at any position of the angular interval 2π , covered by the detector ring. The scattering angle is the same for all detectors ($2\theta = 90^\circ$). The sample to be investigated is placed in the center of the ring and is rotated in the goniometer, which accepts of the apparatus up to 30 kg mass, around the horizontal Z axis arranged at angle of 45° to the incident neutron beam.

The SKAT spectrometer has advantages as compared with other similar instruments:

- Diffraction peaks corresponding to a specific d_{hkl} value, are recorded by all detectors in the same position (time-of-flight channels) in all diffraction spectra obtained from the measured sample. Therefore, there is no need to introduce corrections which depend on the scattering angle and the wave length;
- since the angular range of the detector set up is 180° , it is sufficient a single sample revolution on a goniometer to measure the complete the pole figure;
- important is that various systems such as heaters, high-pressure chambers, devices creating electrical and magnetic fields, etc. can be placed around the sample in the center at the SKAT detector ring.

The main advantage of TOF diffractometers and SKAT included is in a possibility to record different pole figures in simultaneously in a reasonable time. This is especially important for making the texture measurements of the low-symmetry and multiphase geological materials [Feldmann *et al.*, 1991; Ivankina *et al.*, 1999b].

A high-resolution neutron spectrometer NSHR [Walther *et al.*, 1993b] which was used for the texture measurements starting from 1998 is arranged on the same beam at the IBR-2 pulsed reactor in Dubna. Presently a upgrading is going on the NSHR diffractometer as it is necessary to extend the texture measurements of the geological samples.

The ROTAX instrument installed at the ISIS pulsed spallation source in the Rutherford-Appleton laboratory (Great Britain) has been operated for several years as a multi-purpose powder and texture diffractometer outfitted with position-sensitive JULIOS detectors. Functioning as an angle-dispersive TOF diffractometer with the time-of-flight path of about 15 m permits to use the polychromatic neutron spectrum effectively. It should be noted that, combination of a white beam TOF method and the use of the linear detector pursue two goals simultaneously: 1) to reduce the number of rotations of the sample during scanning of the pole figure, 2) to measure simultaneously a great number of the pole figures with different (hkl).

The texture analysis using TOF method and two-dimensional detector system was made at the LANSCE pulse neutron source in Los Alamos (USA) and IPNS of the Argonne National laboratory (USA). Various pole figures are scanned due to different positions of the sample on diffractometers, which were originally designed for diffraction on monocrystals and supplemented with a goniometer and two-dimensional detectors.

A HPPO (High Pressure – Preferred Orientation) diffractometer for measurement of the preferred orientation at high pressure was actually put into operation in Los Alamos [Ben-nett *et al.*, 1999]. The high-intensity TOF diffractometer has a short time-of-flight path (9 m) and it will be used mainly for investigations at high pressure and for the texture measurements. It exhibits a new three-dimensional arrangement of the detector banks with 1400 helium tubes located on five conic rings corresponding to a position at angles of $2\Theta = 10^\circ, 20^\circ, 40^\circ, 90^\circ$ and 150° . The measured interplanar spacing ranges from 0.5 to 9.0 Å. A conventional three-axial goniometer using with the Kappa geometry was used for standard texture measurements. A device for changing position of the sample (32 positions) permits to make the texture analysis of a multiphase sample in a fast way and this is important for systematic investigations of large groups of the geological samples.

The systems surrounding the sample are made specially to study the samples at a wide range of temperature ($4K < T < 200K$) and pressure ($0.1 \text{ MPa} < P < 20 \text{ GPa}$). A three-dimensional arrangement of the detector system of the diffractometer covers a considerable area of the sample surface. In spite of a large size of the surrounding devices, a high density of the neutron flux from the source (a spallation target of the proton storage ring) allows to measure the samples in relatively short periods of time.

Along with the study of the texture changes in materials at different thermodynamic parameters, structures of the substance, internal stresses, magnetic properties of different materials etc. are also studied on the diffractometer. Spallation in a wide pressure and temperature range will make it possible to conduct *in situ* dynamic measurements of chemical reactions, deformations and recrystallization processes.

The study and determination of the crystallographic textures in the research center of the Argonne National laboratory (USA) is done with the help of the general purpose powder diffractometer (GPPD) at the intensive pulse neutron source (IPNS). Design of the instrument and different component facilities allow to solve a rather wide spectrum of material science problems. A moving multidetector system of the diffractometer assists to study with a rather high accuracy the structural parameters, microstresses and textures of materials. There is also possible to carry out experiments with heaters and high-pressure chambers. An extensive biological shielding and the relatively remote location of the instrument allows to work even with highly radioactive samples.

Till today, information regarding possibilities of neutron diffraction in the texture analysis of rocks is not so widespread among geologists and geophysicists. The reason is in a limited number of neutron diffractometers and in a restricted time for measurement, especially if a large collection of samples is to be analyzed. Further efforts are necessary to propagate technology acquired by crystallographers and materials technologists over many years in the field of the quantitative texture and strain/stress analysis and its application in geosciences.

II. Textures and Physical Properties of Rocks and Meteorites

2.1. Textures and Elastic Properties of Rocks at High Hydrostatic Pressures

As has been already mentioned in chapter 1.1., anisotropy of the rocks is dictated by the conditions, which were established at different depths, and by structure of the rocks, for example, by the crystallographic texture. Formation of the crystallographic texture, in its turn, is connected with certain physical processes in the lithosphere, such as plastic deformation, creep, recrystallization etc.

Ivankina *et al.*, [1999a] have started a complex investigation of factors, which influence the elastic anisotropy of the mantle rocks at different hydrostatic pressures. The neutron diffraction texture analysis by the NSHR diffractometer and ultrasonic measurement of the longitudinal wave velocities on spherical samples were employed for the purpose. Later these studies were continued with the SKAT [Nikitin *et al.*, 2001a].

Some results obtained with the SKAT diffractometer for some samples of xenoliths and dunites taken from different regions of Europe. The samples tested were mainly single-phase rocks formed by forsterite (olivine). Specific data about composition, samples locations and origin of the samples are in the paper [Nikitin *et al.*, 2001a].

A quantitative texture analysis of the samples was made on the basis of neutron-diffraction measurements of the xenoliths and dunites samples and of a set of experimental pole figures. Using ODF the pole figures for the main crystallographic planes (100), (010) and (001) were calcu-

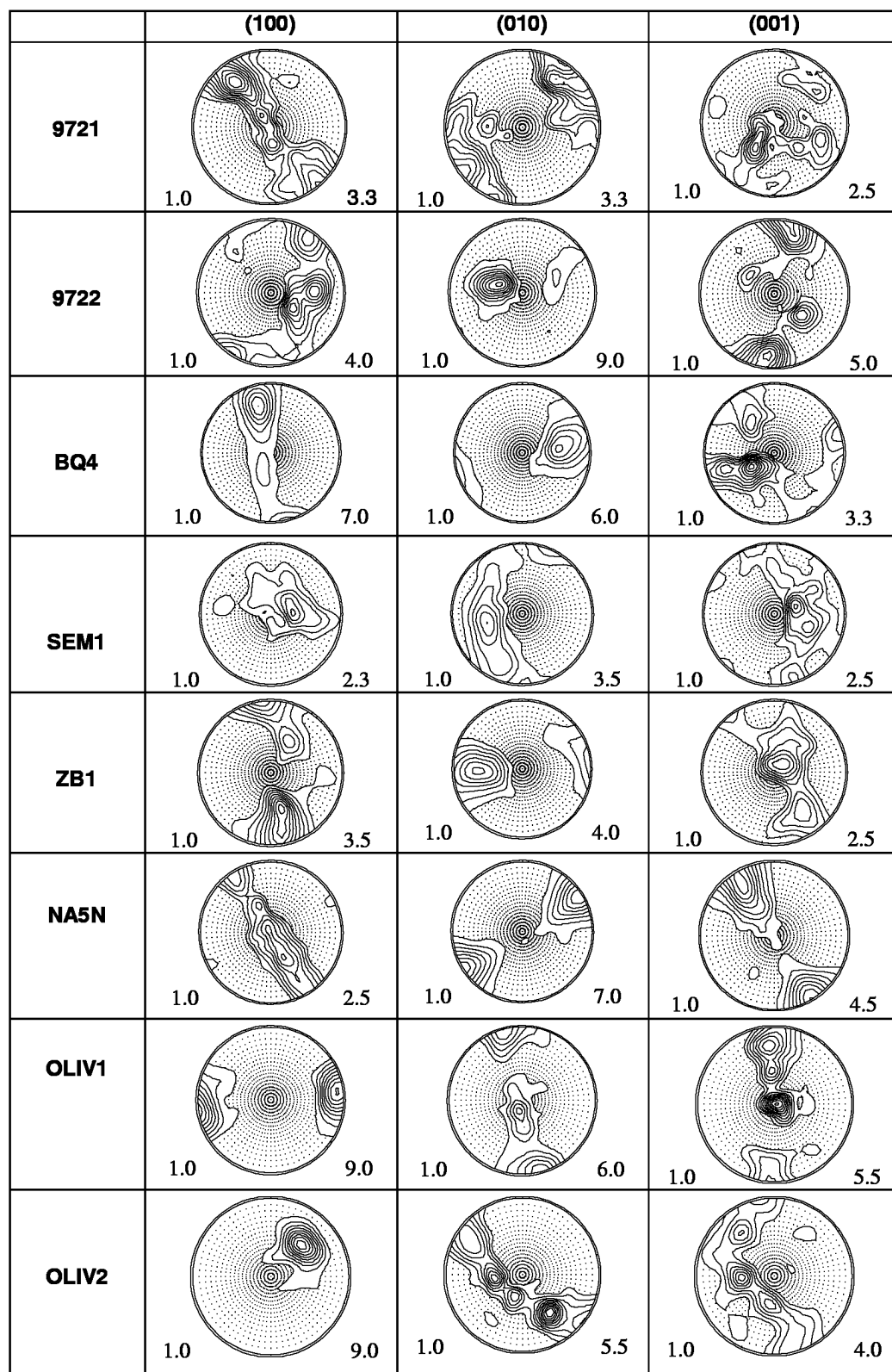


Figure 2. Pole figures of the main crystallographic planes of olivine in respect to the laboratory coordinate system.

Note: Some results are obtained with the SKAT diffractometer for samples of xenoliths and dunites taken from different regions of Europe. Olivine samples from Železny Brod (Czech Republic), Ivrea Zone (Italy), Albania and Norway were collected by scientists from the Geophysical Institute AS CR Z. Pros and others. Xenoliths from Lanzerote Island (Canary Islands) have been kindly granted by A. F. Grachev.

lated (Figure 2), which describe the preferred orientations connected with the extreme directions of the elastic wave velocities in the olivine crystal.

The preferred orientations of planes (100) in samples 9721, 9722 (Ivrea zone, Italy), BQ4 (Albania) and NA5N (Norway) are represented as belts with well expressed maxima distributed along the belts. A rather compact maximum with a high pole density is observed on the (010) pole figure. The pole figures (001) are characterized by a complicated configuration of isolines with several overlapping maxima.

Quite different pattern is observed in the xenolith samples OLIV1 and OLIV2 (Canary Islands). High intensity compact maxima on the (100) pole figures are typical for texture of these samples, while orientation of the (010) and (001) base planes originates or has a tendency to originate of belts with a pronounced pole density maximum.

Texture of olivine in xenoliths SEM1 and ZB1 (Železny Brod, Czech Republic) is less sharp then in xenoliths from the Canary Islands, thus affecting values of the maximum pole density on the pole figures and it is more fuzzy, though pole figures of samples display the similar configuration of isolines.

The quantitative information about texture in terms of ODF, restored from the diffraction data, allowed to simulate of the elastic wave velocity in the polycrystalline olivine samples having a crystallographic texture [Nikitin *et al.*, 2001a]. This simulation implied the calculation of elastic stiffness tensor of polycrystalline sample by the known averaging methods based on the ODF and elastic modules of the olivine monocrystal as well as construction of the stereoplots reflecting spatial distribution of velocities on P-wave in the sphere. Tabulated values of components of the olivine elastic constant tensor are taken from [Simmons and Wang, 1971].

The computed maps of isolines of the spatial distribution of the P-wave velocities in the coordinate system corresponding to the position of the sample in the diffraction experiment are shown on Figure 3.

Velocities of the longitudinal elastic waves at different confining pressures were measured for the same samples by the ultrasonic method [Pros, 1977]. The method is, that emission and reception of the ultrasonic pulses is effected by two piezoelectric transducers having a point contact with the same surface, in different directions along the diameter of the spherical sample. The electroacoustic transducers move in the plane passing through the axis of rotation. The proposed system permits to measure the elastic impulse travel time in any direction and to calculate velocities. When the sample rotates discretely at a step of 15° one obtains a set of 150 points, which are marked stereographic grid related to the coordinate system of the spherical sample. It should be noted, that orientation maps of the elastic P-wave velocity and pole figures from the diffraction experiment are constructed in the same coordinate system.

Velocities of the longitudinal elastic wave were measured in a cyclic way: first, at the atmospheric pressure; then at the pressures of 10, 20, 50, 100, 200, 400 MPa and in the reverse order with exactly the same values on the load scale [Ivankina *et al.*, 1999b; Locajicek *et al.*, 1999; Nikitin *et al.*, 2001a].

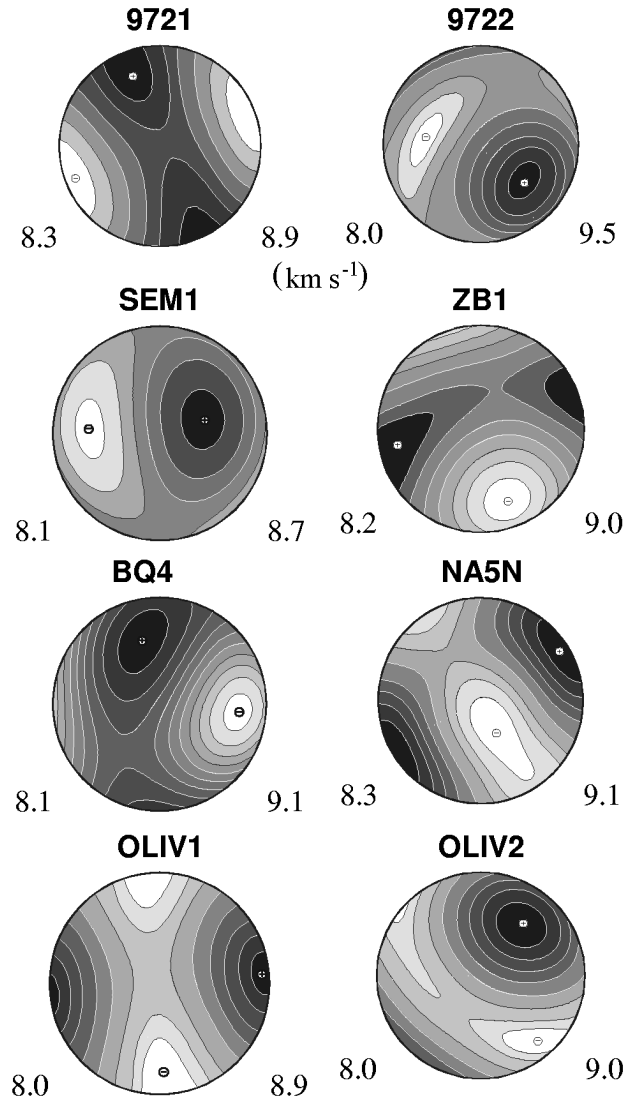


Figure 3. Modeled bulk-rock P-wave velocity distributions calculated from ODF's.

Maximum and minimum velocities of the longitudinal waves as well as anisotropy factors, which were calculated by the following formula, are given in Table 2

$$k = (V_{P \max} - V_{P \min}) / V_{P \min} \times 100\% . \quad (15)$$

It is seen from Table 2 that the investigated samples at the atmospheric pressure are characterized by a high anisotropy of the P-wave velocities. The anisotropy factor of samples 9721 and 9722 practically does not change along with increasing pressure. Such behavior of samples is confirmed by the dependence of the anisotropy factors of the P-wave velocities k upon hydrostatic pressure (Figure 4). The elastic anisotropy of various samples differs significantly with the hydrostatic pressure rise. Dunite samples 9721, 9722 and BQ4 form one group whose anisotropy factors do not change practically with the pressure increasing, and xenolith samples SEM1 and ZB1 demonstrate decrease of the anisotropy

Table 2. Experimental values of longitudinal elastic wave velocities and their anisotropy k at different confining pressures

Sample	Pressure, MPa	V_p max, km/s	V_p min, km/s	k , %
9721	0.1	8.0	7.0	14
	100	8.2	7.3	12
	400	8.3	7.5	11
9722	0.1	9.4	7.6	24
	100	9.4	7.8	21
	400	9.6	7.8	23
BQ4	0.1	8.2	6.9	19
	100	8.8	7.9	11
	400	8.9	8.0	11
SEM1	0.1	6.5	6.0	8
	100	7.4	7.1	4
	400	7.9	7.5	5
ZB1	0.1	5.8	4.7	23
	100	7.8	7.3	7
	400	8.3	7.6	9

k at pressures up to 100 MPa followed by its monotonous increasing.

Figure 5 shows maps of the P-wave velocity isolines, constructed from experimental data, obtained at 0.1, 100 and 400 MPa for the same samples which reflect a spatial variations of the elastic anisotropy with pressure increasing. Dunite samples 9721 and 9722 have stable patterns of the P-wave velocity distribution throughout the hydrostatic pressure range. For sample BQ4 configuration isolines changes with the increasing of pressure, directions of the velocity maximum and minimum (to a greater extent) on the stereographic projection are shifted, but the pattern basically stabilizes. The counter maps of the samples ZB1 and SEM1 (Figure 5) show no regular distribution at atmospheric pressure. With the pressure rise the isolines acquire a more perfect and symmetric configuration. Positions of the velocity maxima and minima are shifted and in case of sample ZB1 they are switched. With a further pressure rise from 100 up to 400 MPa the spatial distribution of velocities become more smooth.

The model distributions V_p (Figure 3) obtained from the ultrasonic experiment at 400 MPa (Figure 5). This fact provides evidence that elastic anisotropy of these rocks at high pressure is mainly controlled by the crystallographic olivine texture. Nevertheless, some difference in the model and experimental patterns concern the maximum and minimum velocities and elastic anisotropy k . Only one factor having influence on the elastic anisotropy of the bulk sample of dunite or xenolith – crystallographic texture was taken into consideration in simulation of the P-wave velocity distribution. Evidently, influence of the form texture (presence of the oriented cracks, intergranular boundaries etc.) or vice versa, presence of the random oriented defects even at a

high uniform pressure might cause of anisotropy increasing, induced mainly by the crystallographic texture, as well as its decreasing.

2.2. Textures and Piezoelectric Properties of Rocks

The volumetric piezoelectric effect in rock occur if, in addition to preferred orientations of the electric axes of crystals, these axes have orientational polarity (Figure 6).

The first statement about existence of piezoelectric properties of rocks appeared in the work of M. P. Volarovich and E. I. Parkhomenko [*Volarovich and Parkhomenko*, 1954]. The nature of the piezoelectric effect of polycrystals (rocks in particular) was explained on the basis of the piezoelectric texture theory which was developed by A. V. Shubnikov [*Shubnikov*, 1946].

The first prove of the piezoelectric effect of rocks was the change of sign of the polarized charge at the change of the loading sign which was typical for the piezoelectric crystals only. Tests of polycrystalline rocks as well as single crystals of quartz by applying compression and extension alternatively show the change of the charge sign. Upon excitation of the piezoelectric effect by ultrasound phase change of e sample mechanical oscillation into π the same change of phase of electrical oscillations is observed.

Additional evidence for piezoelectric nature of the effect is establishing of the inverse piezoelectric effect which was observed when the rock sample was used as an ultrasonic emitter; ultrasonic oscillations were recorded when electric signal was applied to the sample. Authors [*Nikitin and Parkhomenko*, 1982; *Nikitin et al.*, 1981] have developed an experimental procedure to determine the texture induced piezoelectric effect in polycrystals. The procedure is based on the fact that piezoelectric materials possess a regular (dictated by symmetry of piezoelectric properties of material) distribution of polarization charge density over the sample surface under the static loading (or dynamic excitation). The comparison of experimentally measured angular

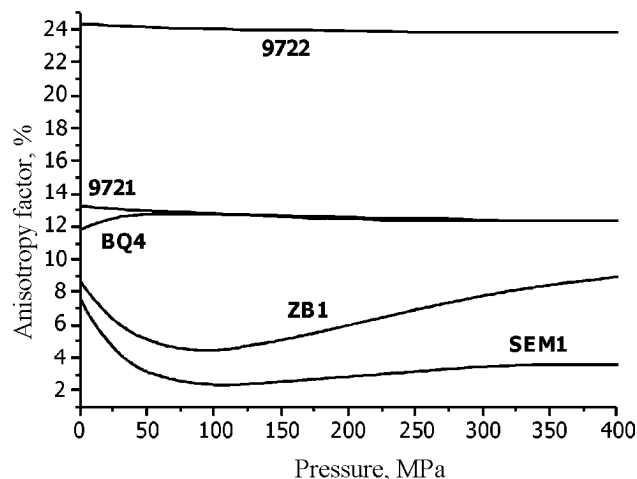


Figure 4. Dependence of elastic anisotropy of samples on confining pressure.

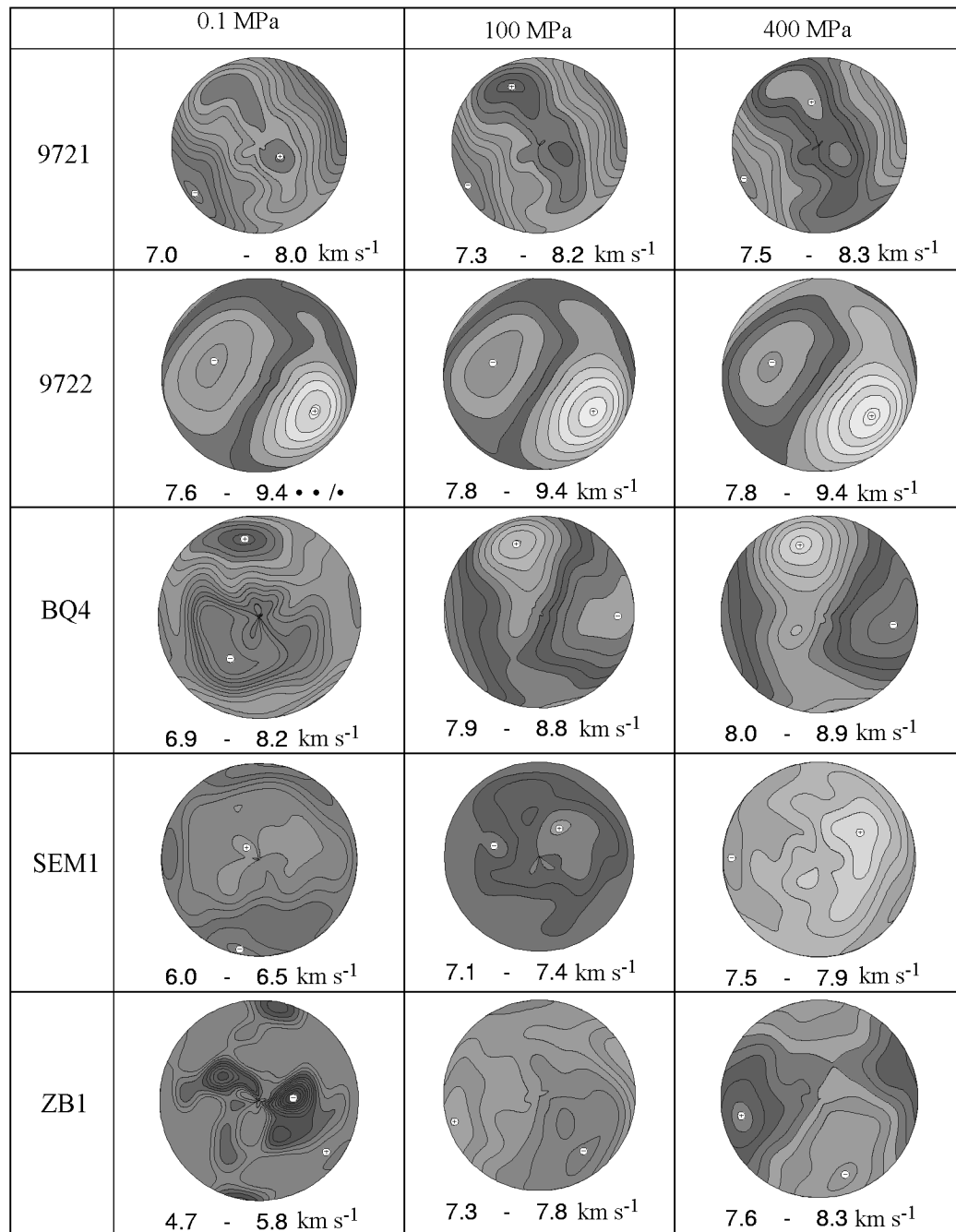


Figure 5. Maps of isolines of longitudinal elastic wave velocity distribution of olivine samples at atmospheric pressure and at confining pressures of 100 and 400 MPa.

dependencies of the effect in the samples with theoretical cross-sections of the indicative surfaces permits to ascertain the texture-induced piezoelectric effect and to determine the symmetry type of piezoelectric properties.

Studies containing quite new information about textures of piezoelectrically active samples appeared in recent years by using neutron diffraction that presents the most comprehensive information regarding large polycrystalline samples. A sample of the veined quartz showing a high piezoelec-

tric activity was analyzed in the work of [Ivankina *et al.*, 1991; Walther *et al.*, 1990]. The pole figures were measured for this sample by the time-of-flight method on the neutron spectrometer NSHR (JINR, Dubna). The symmetry of the pole figures was either of the sixth or third order (Figure 7).

Afterwards, angular dependencies of the piezoelectric field (Figure 8) were recorded by an electromagnetic method using point movable electrode at ultrasonic excitation of the sample [Nikitin *et al.*, 1981]. The analysis of the neutron

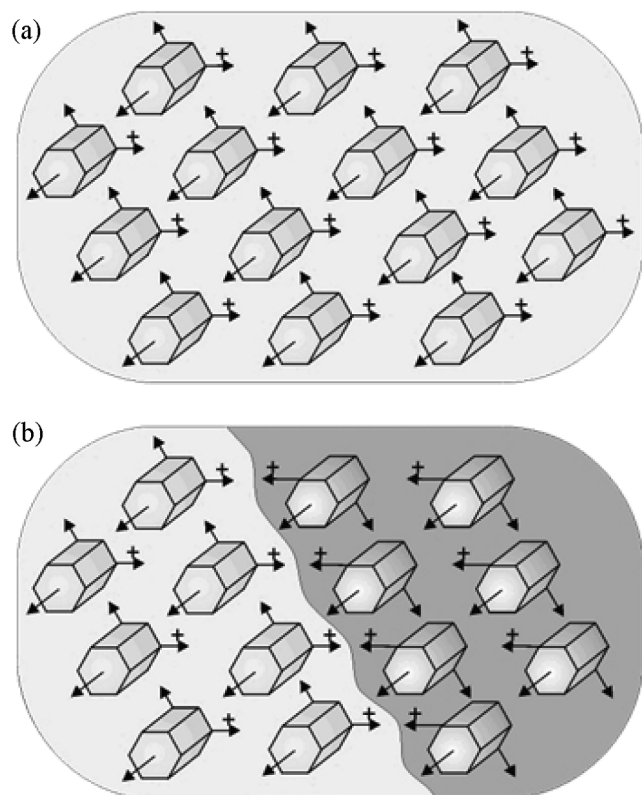


Figure 6. Models of ideal texturized vein quartz which is a) piezoelectrically active, b) piezoelectrically neutral.

diffraction and electrometric measurements allowed to conclude that distribution of the pole density lines on the pole figures is in a good agreement with the structure and properties of the piezoelectric field of the sample. The experimental data presented convincingly demonstrated the piezoelectric

activity of rock as a result of its specific texture.

Some geophysicists did not accept explanation of the piezoelectric effect in rocks based on theory of A. V. Shubnikov. The research workers [Tuck *et al.*, 1977] tried to interpret the piezoelectric properties of rocks due to presence of large grains without non compensated electrical charge or due to a statistic effect. J. Bishop was the first [Bishop, 1981] who confirmed by experiments on the volume representative cubic samples the existence of piezoelectric effect due to textural features of rocks formed by minerals with piezoelectric properties. Using the supplementary experimental studies the authors [Ghomshei and Templeton, 1989] examined the piezoelectric data obtained on the cubic veined quartz samples taken from different points of the veined surface; the results of the neutron diffraction investigation of the same samples were also used. Measurements of piezoelectric effect of the veined quartz have clearly confirmed its structural origin; the measured value was greater than the expected statistical effect. The texture measurements by the neutron diffraction revealed a regular preferred orientation of the a-axes of quartz which determines the piezoelectric effect of the bulk rock sample.

Explanation of physical mechanisms and processes, which lead to formation of rocks possessing piezoelectric properties in the earth's crust under natural conditions, is an important and, evidently, finally unsolved problem. Three inferences were put forward about a physical mechanisms of the formation of piezoelectric active rocks with textures in the [Nikitin, 1996; Nikitin and Ivankina, 1995]. The first is related to the origination of piezoelectric properties in the growth textures due to a phenomenal feature of quartz, namely anisotropy of the single quartz growth rate along the electric axes direction. Another scenario suggests that preferred orientations were originated in the β -quartz under various deformation conditions (shear or triaxial loading) as a result of the high-temperature plastic deformation in quartz [Walther *et al.*, 1993a]. With temperature continuing to fall below 573° at

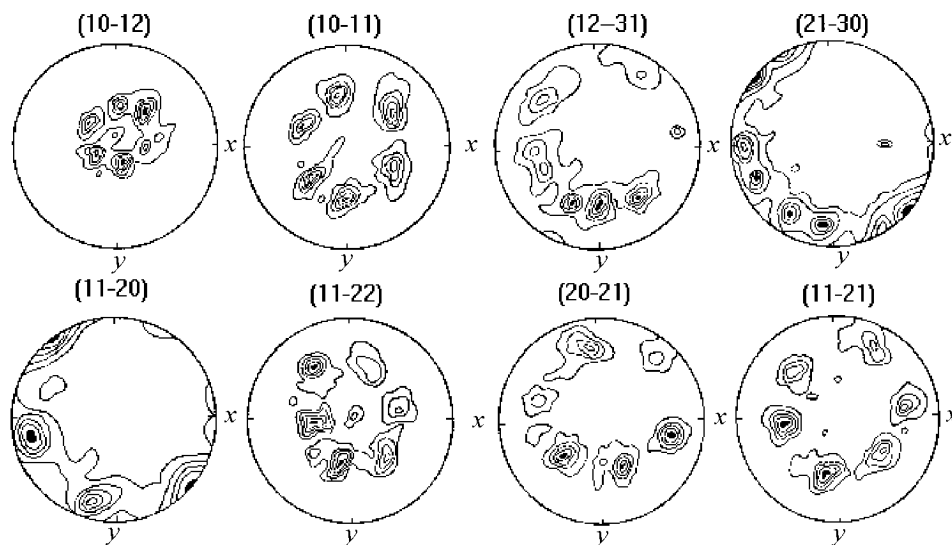


Figure 7. Pole figures of quartz measured by neutron diffraction at the NSHR spectrometer.

the β - α phase transition to polycrystalline quartz aggregate become piezoelectrically active. Finally, the author [Nikitin, 1996] has made a supposition that piezoelectric activity of the sedimentary rock is possible, for example, under a long-term stationary electric field within ancient basin or due to a source causing self-polarization of the settling piezoelectric active particles.

2.3. Textures and Magnetic Properties

All the rockforming minerals may be divided into diamagnetics, paramagnetics and ferromagnetics. The anisotropy of magnetic susceptibility (AMS) of the bulk rock sample is a superposition of magnetization vectors of all the mineral components of the rock. The degree of anisotropy is determined by the anisotropic properties of the rock-forming minerals [Hrouda, 1982], shape of grains [Uyeda *et al.*, 1963] and crystallographic texture of the mineral phases [Hrouda *et al.*, 1985].

The anisotropy of magnetic susceptibility (AMS) of material relates the magnitude applied external magnetic field H with the induced magnetization M of the material by

$$M_i = k_{ij} H_j, \quad (16)$$

where k_{ij} – proportionality factor which is the second-rank tensor. The bulk susceptibility k ($k = (k_{\max} + k_{\min} + k_{\text{int}})/3$), which is determined as an arithmetic mean of the three main axes k_{\max} , k_{\min} and k_{int} of the AMS ellipsoid, is a parameter used to represent AMS.

Parameters which are usually used to establish the AMS differ from those used for measurement of the pole figures by diffraction methods or by some other non-magnetic methods. The so-called orientation tensor is employed to compare the AMS method with other non-magnetic methods. The main problem is in converting the magnetic susceptibility tensor into the orientation tensor for rocks whose magnetic anisotropy is conditioned by minerals with the uniaxial magnetic anisotropy (phylosilicates, hematite, pyrrhotite) [Hrouda and Schulmann, 1990]. The method of determining the orientation tensor from the AMS is possible, provided the following conditions are fulfilled:

- AMS of the rock exists only due to identical minerals with a known uniaxial grain anisotropy;
- grains of this mineral are identical in size;
- grains do not interact with magnetic fields of their own.

Consequently, the method cannot be used to determine the orientation tensor of the rocks, with the AMS conditioned by magnetite, as its grains reveal usually a triaxial anisotropy (because of the grain shape effect) and the grain anisotropy extent varies from grain to grain in accordance with the shape variation. The method is more applicable to rocks with the AMS conditioned by pyrrhotite, hematite, mica or chlorite, as a magnetocrystalline anisotropy, which does not depend on the mineral shape and remains constant from grain to grain, is observed in these minerals [Uyeda *et al.*, 1963].

One of the most important problems of the structural geology is related to the magnetic susceptibility source, i.e.

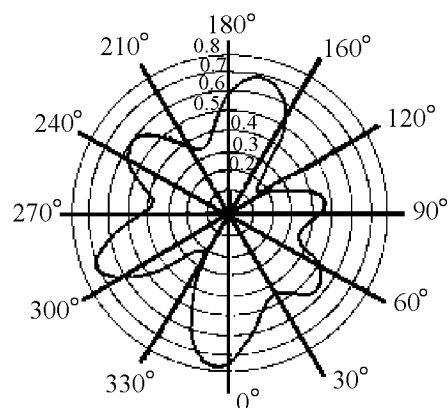


Figure 8. Angular dependence of electric field potentials (mV) recorded in a vein quartz. Cylinder axes is normal to the plane where preferred orientation of crystallographic axes (11–20) is observed.

with establishing the quantitative relation of the magnetic structure to the rock structure. The anisotropy of magnetic susceptibility (AMS) of the bulk rock sample increases notably due to presence of minerals such as magnetite, pyrrhotite or hematite. Typical values of the magnetic susceptibility of such ferromagnetic materials are of the order of $5\text{--}6 \times 10^{-3}$ SI volume unit. Magnetite is a mineral where the AMS depends mainly on the grain shape. The AMS of other ferrite minerals is controlled by the crystalline lattice type.

Simulation of the c-axes pole figures of the hematite rock was conducted and the relevant AMS-diagrams were calculated to establish interrelation between the hematite texture and its magnetic structure [Siemens *et al.*, 2000]. It turned out that quite different pictures of the preferred orientation of the hematite c-axes are characterized by the identical magnetic parameters. Consequently, knowledge of the AMS anisotropy of the texturized samples does not allow to judge the type of their crystallographic texture. Further a comparison was made in the paper between the experimentally measured anisotropy of the magnetic susceptibility, hematite pole figures assured by neutron diffraction and theoretical AMS data obtained on the basis of the texture analysis. The conclusion speaks about necessity to supplement a low cost AMS investigation method with the results of more accurate neutron diffraction or X-ray measurements on the same geological samples so as to obtain a more comprehensive and quality knowledge of the magnetic properties of the texturized rocks.

The majority of the rockforming minerals are paramagnetics and diamagnetics. The magnetic susceptibility value of the diamagnetic minerals is 1×10^{-4} SI volume unit; in case of the paramagnetic minerals this value is negative -1×10^{-5} SI volume unit.

It has been found by Rochette, [1987] that the crystallographic texture of the paramagnetic minerals for rocks possessing a weak anisotropy of magnetic susceptibility may contribute considerably into anisotropy of magnetic properties of the bulk sample. The texture based calculations of

the AMS were made in the paper [Siegsmund *et al.*, 1995], where a quantitative relation was found between the preferred orientations of mica and the magnetic structure of different types of the mica-bearing rock (orthogneiss, granulite, mylonite).

A magnetic texture of the volcanic lava in the Kazbegi region (North Caucasus) has analyzed in the paper by [Asanidze *et al.*, 2001]. The data cited indicate to the fact that on the one hand the magnetic texture was formed when the lava was still moving, on the other hand, the NRM appeared when the stream became hard and its temperature was decreased below the Curie point of the magnetic minerals.

The above studies have shown that the multiphase rocks have a common problem caused by interaction and interosculation of structures of different mineral components. The problem may be resolved in a simple way by a selection of samples where only one mineral is the carrier of the AMS. However, identification of this mineral presents certain problems with other minerals ignored. Thus, a small quantity of neglected magnetite, which exists in numerous types of rock, may influence upon the investigation results. To solve this problem the samples must be analyzed with the altering magnetic fields to separate anisotropic components obtained from individual minerals. However, nothing has been mentioned in literature about such AMS experiments with the multiphase rocks. The problem of finding the preferred orientations of the main rockforming minerals with a subsequent simulation of the AMS data can be resolved with success using of the neutron diffraction texture analysis.

Beside of quartz and feldspar, calcite is the most essential rockforming mineral showing diamagnetic properties. It was shown in investigation [de Wall *et al.*, 2000] that value and direction of the AMS-ellipsoid principle axes may be calculated with a good accuracy on the basis of the neutron diffraction measurements of the coarse-grained marble (Dubna, Russia). Certain difference between the calculated AMS an results of the experimental measurement of the magnetic susceptibility of the same samples may be due to lack of possibility of accounting for the grain size and grain shape during AMS simulating.

2.4. Textures and Thermal Properties of Rocks

The textures of the polycrystalline materials, formed by crystallites with a non-cubic lattice, cause anisotropy of the thermal properties, especially thermal conductivity and thermal volume expansion.

The thermal conductivity of rocks belong to the main parameters which are required for determination of the geothermal fields. Thus, the thermal conductivity and temperature gradient values are used for estimation of the heat flow density in the interior of the Earth. The thermal conductivity of rocks in the Earth's crust depends on pressure, temperature, mineral composition and on the type and the fluid saturation degree.

The experimental results with the paragneiss sample extracted from the core of the superdeep borehole KTB may

serve as an example of investigation of the texture influence on the thermal conductivity anisotropy [Siegsmund, 1994]. The thermal conductivity values were obtained for three mutually perpendicular directions at a room temperature and at a pressure rise up to 60 MPa. To estimate the contribution of each paragneiss mineral component (quartz, plagioclase and muscovite) to the meaning anisotropy of the measured thermal conductivity was compared with the similar values of the mineral components which were calculated by averaging methods. The thermal conductivity of a compacted (without cracks) polycrystalline aggregate under dry conditions depends on the thermal conductivity of the single crystal, on the crystallographic preferred orientation and on the volume fraction of the constituent minerals. The interaction of the texture-dependent thermal conductivity of quartz, mica and plagioclase demonstrates a complicated nature of the rock thermal conductivity. It turned out, that superposition of the quartz and mica textures with almost isotropic plagioclase produces a strong anisotropy of thermal conductivity (about 32%). The thermal conductivity data obtained at the time of drilling the superdeep borehole KTB support the results of simulation.

It should be noted that representation of results obtained in the work [Siegsmund, 1994] is insufficient. The measured quartz texture is described as weak, though the density on the (0001) pole figure is not given. As to sharpness of the mica texture one has only to guess. The numeric results on a spatial distribution of the coefficient of thermal conductivity λ , calculated on the basis of data quartz and mica textures, are not available. Moreover, the up-to-date methods of simulation of the physical properties permit to obtain the pattern of the spatial distribution of the texture-dependent property of bulk sample, are also not available in the work cited.

If the quantitative texture analysis of the rock samples was made in detail, computation of the coefficient of thermal expansion α is possible according to the ODF data and the α value of single crystal. Similar simulation allows to estimate the correlation of the crystallographic texture with the type of the thermal expansion coefficient tensor. The works about influence of the crystallographic texture on the thermal expansion of the natural marble samples are well known [Leiss and Weiss, 2000; Siegsmund *et al.*, 1997, 2000].

Marble as a building material has been used for over 2000 years. Buildings and other structures made of marble are subject to a mechanical (thermal expansion/contraction cycles) and to a chemical weathering. These processes taken together lead to a considerable rock distribution. The degradation depends not only on the climatic conditions, but also on the mineralogical, chemical features and fabric of the rock. It has been also shown, that the thermal expansion of marble depends on the type and degree of the preferred orientation of the strongly anisotropic calcite grains [Siegsmund *et al.*, 1997].

Besides of the crystallographic texture the following factors influence on the thermal properties of marble: defects of the rock fabric, grain size, grain size distribution, grain shape, geometry of the grain boundaries and other features of the shape texture. The marble samples from the Carrara, analyzed in the work by [Widhalm *et al.*, 1996], have revealed a strong anisotropy of the thermal expansion,

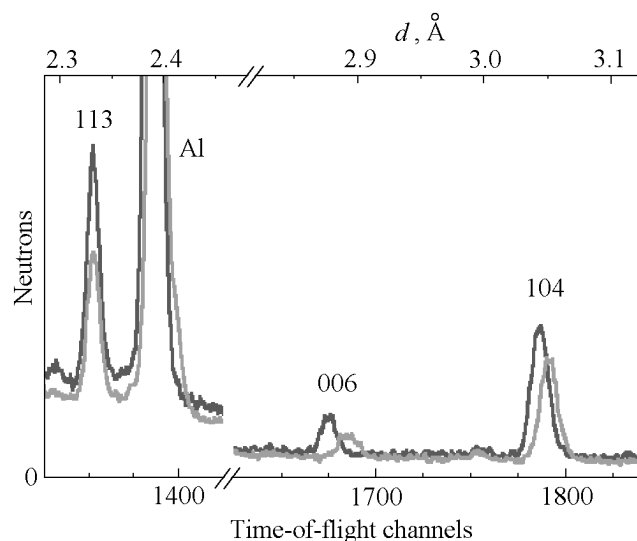


Figure 9. Parts of the calcite diffraction spectra, recorded at 20°C and 220°C.

although the crystallographic texture of these samples is not well developed and sharp. The anisotropy of this marble is due to a strong grain anisotropy and to orientation of the grain boundaries.

It was confirmed by *Leiss and Weiss*, [2000] that the spatial distribution of the thermal expansion is controlled mainly by the texture. This was done with the Carrara marble samples using model calculation of the thermal expansion coefficients on the basis of the restored ODF. At the same time, disagreement between values of the model thermal expansion coefficients calculated from the crystallographic texture only and those measured experimentally is a result of influence of the other structural parameters and shape texture. On this basis the authors came to a conclusion that correlation between the crystallographic textures and thermal properties is not sufficient for understanding of degradation mechanisms of marble.

Samples of calcite-bearing rocks (similar to marble) frequently reveal a strong preferred orientation of grains. Calcite is characterized sufficiently ductile behavior as compared with other minerals, therefore, the calcite-bearing rocks are a good model for the rock deformation experiments. The abnormal behavior of physical properties of marble caused by an external loading and temperatures was discovered by the authors [*Ivankina et al.*, 1998, 2001]. The experiments were conducted with the help of the TOF-diffractometer SKAT equipped with a high temperature chamber for the uniaxial compression (Dubna, Russia). There is a possibility to calculate from the diffraction spectra, microdeformation and thermal characteristics of calcite at different temperatures in the course of a mechanical loading or heating.

Anisotropy of the calcite thermal expansion coefficient shows itself in the difference of the tensor components in terms of value and sign. It is notable that only calcite and otavite have negative thermal expansion coefficients, while the other carbonates possess only positive thermal expansion coefficients.

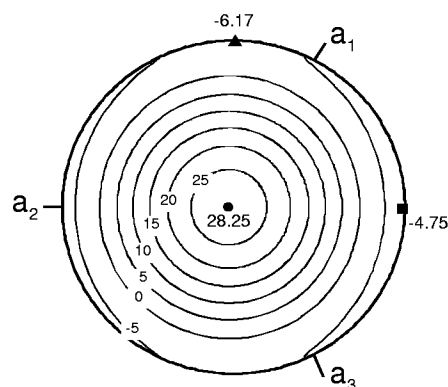


Figure 10. Spatial distribution of the thermal expansion coefficient α [10^{-6} K^{-1}] of the calcite single crystal, calculated from the (0006), (10-14) and (11-23) peak shifts on the diffraction pasterns.

Displacements of the Bragg fabrics different in their value were observed on the diffraction patterns due to anisotropy of calcite at the temperature rise (Figure 9). The greatest displacement was recorded at the (0006) peak. It made $1.79 \times 10^{-2} \text{ \AA}$ within the temperature range of 20 to 220°C that corresponded to a relative lattice deformation $\Delta d/d = 6.20 \times 10^{-3}$. The time-of-flight diffraction spectra measured at different temperatures permitted the spatial distribution of the thermal expansion coefficient α to be calculated on the basis of displacements and relative lattice deformations of different planes of calcite lattice. A spatial distribution of α has an axial symmetry (Figure 10). The maximum value of the main component of tensor $\alpha_{\max} = 28.25 \times 10^{-6} \text{ K}^{-1}$. Since the principle axis of the tensor coincides practically with the direction of the normal to the (0006) plane, difference between the minimum value of the main component of tensor $\alpha_{\min} = -4.75 \times 10^{-6} \text{ K}^{-1}$ and intermediate $\alpha_{\text{int}} = -6.17 \times 10^{-6} \text{ K}^{-1}$ indicates the experimental error which was about 5% as a result of calculation.

2.5. Investigation of the Structure, Texture and Properties of Meteorites

Shortly after an iron meteorite has fallen near Sterlitamak in Baskiria its fragments were subjected to a texture analysis [*Helming et al.*, 1991]. The pole figures measured presented information about the deformation texture, which most probably occurred when a strongly heated meteorite hit upon the Earth's surface.

The study on detection of tracks of the fast heavy nuclei was another investigation with the use of the neutron diffractometry aimed at determination of texture in meteorites was conducted in JINR (Dubna). Setting of this task is related to one of the fundamental scientific directions in the nuclear physics – seeking of the transuranium elements ($Z > 114$) in the primary space substance. The work in the frame of the problem is underway for detection and analysis of the radiation tracks in olivines of meteorites. It is

shown in papers [*Silk and Barnes, 1959; Young, 1958*] that the natural and synthetic ionic and covalent crystals have the property of recording and keeping the microscopic defects of structure which occur therein when heavy charged particles are passing through. The main parameters in the track analysis are geometric characteristics of tracks. The neutron diffraction texture analysis of such objects can give a justified conclusion about their plastic deformation and, thereby, to estimate truth of the track analysis results. It was found on the basis of the texture analysis of the pieces of Maryalahti and Eagle Station meteorites by the pole figures that there were no deformation texture in the olivine component of the samples [*Nikitin et al., 1999*]. Interpretation of data, based on the known physical mechanisms of the deformation texture development in olivinites, gave grounds to make a conclusion about a good preservation of tracks in the olivine crystals which originated upon decay of the uranium group nuclei.

The neutron diffractometry was used for investigation of the meteorite fragments with the object of finding the twinning and the orientation relationships of different phases. The orientation of crystallites in meteorites is observed in the process of cooling after the phase transitions or after a mechanical twinning caused by shock events. The microstructure of three nickel-iron meteorites, two hexahedrons from Walker Country (Alabama) and Coahuila (Mexico) and one octahedron from Gibeon (Namibia) was analyzed on the basis of pole figures with a very narrow scanning net, comprising 7651 different orientations of the sample [*Höfler et al., 1988*].

The pole figures of the BCC-kamacite (t.i. body-centered α -Fe with less than 6% of Ni by weight). Two types of the pole density maxima with a different intensity were observed. The volume content of twins is about 6% and 8% for samples from Walker Country and Coahuila respectively. This was found from the intensity relation of the single crystal and the twin. Whereas the Coahuila meteorite is characterized by a symmetric maximum of the pole density, the Walker Country sample has a more asymmetric shape with several fuzzy extensions. This speaks about presence of several small pieces of kamacite with a weak distinction of orientation which was formed because of breakage inside the meteorite sample.

The octahedron from Gibeon was analyzed for the orientation relationships of taenite (γ -Fe with 30% of Ni by weight) and kamacite. The taenite pole figures have shown that the taenite rims possess a γ -phase orientation of the parent crystal. The kamacite pole figures are characterized by groups and belts having several intensive maxima. Orientation of the kamacite plates and the taenite rims is close to the Nishiyama-Wassermann relationships of ($\{110\}\alpha\|\{111\}\gamma$), $\langle 001 \rangle \alpha \parallel \langle -110 \rangle \gamma$. An alternative case is observed in the kamacite crystals that can be explained by influence of deformation during the crystal growth.

The examples of the neutron investigation of the meteorite substance point to the fact that a conceptual, long-term and a complex program for application of the neutron diffraction analysis to this field of science does not exist. Evidently, enhancement of the use of the neutron physics methods in cosmology might be implemented, provided the co-operation of the Russian and international experts on the

structure and evolution of the solar system, on meteorites and on the neutron physics is established.

III. Use of Data on the Rock Textures in Resolving the Problems of Geology and Geophysics

3.1. Investigation of Metamorphic, Geodynamic and Evolutionary Processes from Data on Textures of Multiphase and Deep-Seated Samples

The study of structure, regularities of rocks at different levels is the fundamental problem of geology. One of the main tasks in the frame of this direction is the study of regularities and mechanisms of generation of the rock shape and crystallographic textures during magmatic, tectonic and metamorphic processes under the thermodynamic conditions in the lithosphere.

Investigation of relations between features of the textures of different mineral phases of rocks and the physical-chemical mechanisms of metamorphism and other evolution processes, will permit to approach the understanding of phenomena, that, on one hand, modify composition, properties, state of the rocks, and on the other hand, they ensure a striking preservation some of their properties. The essential progress in the solution of similar tasks was as a result of an active application of the neutron diffraction texture analysis in different countries, used together with other physical and petrophysical methods [*Sobolev and Nikitin, 2001*].

Till today the texture analysis of the rocks was conducted mainly on the monomineral rocks, despite the fact that the rock is a multiphase formation, as a rule [*Mainprice and Nicolas, 1989*]. The results of the neutron diffraction texture analysis of the multiphase rock (granulites from the Low Austria) described in the paper by [*Ullemeyer and Weber, 1999*], allow the textures of some rockforming minerals (for example, quartz and biotite) to be treated as indicators of typical stages of the deformation history of granulites. Thus, for example, the predominant orientation of quartz obtained does not fit a usual coordinate system of the sample, which is usually connected with the schistosity directions (or "foliation-lineation") and with the geographic coordinates. Similar deviations in the spatial orientation may be used for estimation of the direction of the large-scale horizontal shear component, which is known from the geological literature as the "transpressive shear vector."

This section covers results of the complex investigation of textures of amphibolites and gneiss is taken from the Kola superdeep bore-hole (the depth of 8.5 to 11.5 km) and their analogues taken from the surface of the Pechenega geological structure. At the same time an attempt was made to trace the sequence of the metamorphic processes that caused the transformation of textures. The samples taken from the depth and the surface (two samples of gneiss, two samples of amphibolite) exhibit identical mineral (Figure 11) and chemical composition and the mineral density.

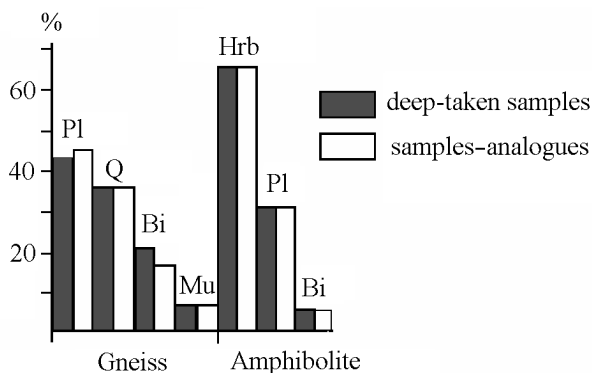


Figure 11. Mineral composition of the Kola samples: Pl – plagioclase, Q – quartz, Bi – biotite, Mu – muscovite, Hrb – hornblende.

Measurements of texture were made by the neutron texture diffractometer SKAT at the pulse reactor IBR-2. Figure 12 shows the time-of-flight diffraction spectrum of sample K9002 gneiss. The texture analysis of such multiphase materials, composed of the low-symmetry minerals, is not trivial as the spectra show a great number of the Bragg reflections from different crystallographic planes, some of which being overlapped. Nevertheless, a sufficient number of the experimental pole figures of plagioclase, quartz and biotite (in the case of gneiss) and the pole figures of the hornblende, plagioclase and quartz (in the case of amphibolites) was retrieved from the diffraction data.

From the set of experimental pole figures the orientation distribution functions (ODF) were restored for the mineral phases dominating in terms of percentage and on their basis calculations were made of the pole figures of the main crystallographic planes (100), (010) and (001) for the hornblende, plagioclase and biotite and planes (0001), (11–20) for

quartz. The texture analysis results indicate to presence of a well developed textures of the main rockforming minerals.

The analysis of the texture found in the hornblende (Figure 13) permits the assumption to be made about existence of two stages in formation of the preferred orientations of this mineral component in amphibolites. Strongly correlating maxima of the main crystallographic planes (001), (010) and (100) are the inherent features of the first stage, whereas the second stage is expressed in girdle distribution of the pole density which is most clearly becomes apparent on the (010) PF.

The preferred orientation of the first type, was generated, evidently, at the earlier stage of the rock formation and is governed by a mechanism of the plastic deformation of the hornblende grains in the direction [001] on the planes (100). This slip system in the hornblende was found experimentally at 600–750°C and at the hydrostatic pressure of 10 kbar. The next stage of evolution of texture which produced the orientation girdles on the PF might be induced, for example, by recrystallization mechanisms.

The fact that the preferred orientation of plagioclase (Figure 14) is more weak as compared with the hornblende texture can be explained by its greater texture to the deformation and metamorphism processes. It is of interest, that a tendency to form the preferred orientations with a strong maximum in the center of the PF is seen on the (100) PF of all the samples. But together with other pole figures, having the girdle with the weak broaden peaks, the plagioclase texture cannot be treated only as a result of the plastic deformation by a dislocation slip.

The fact that the (001) pinacoid planes of plagioclase in the gneiss and amphibolite samples retained their spatial preferred orientation (Figures 14, 15), may indicate in favor of a single orientation mechanism, which generated the plagioclase textures and acted during the geological epoch. The twinning under the plastic deformation conditions could most likely become such a mechanism. The subsequent

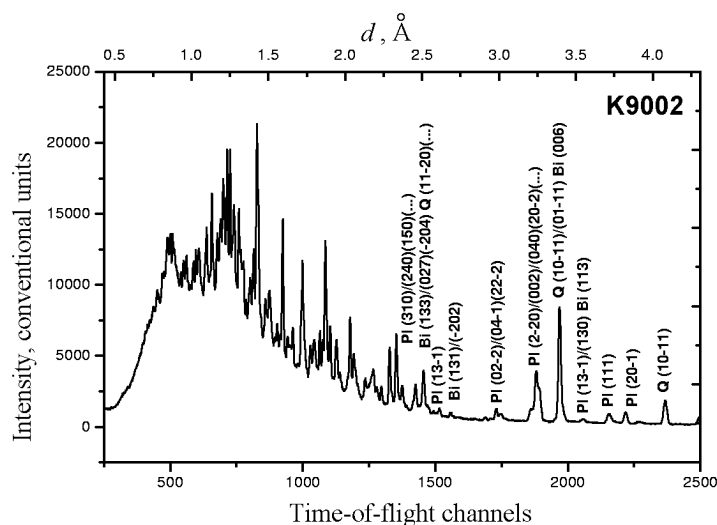


Figure 12. Diffraction spectrum of sample K9002. Some Bragg reflections are indexed thereon Pl – plagioclase, Q – quartz, Bi – biotite.

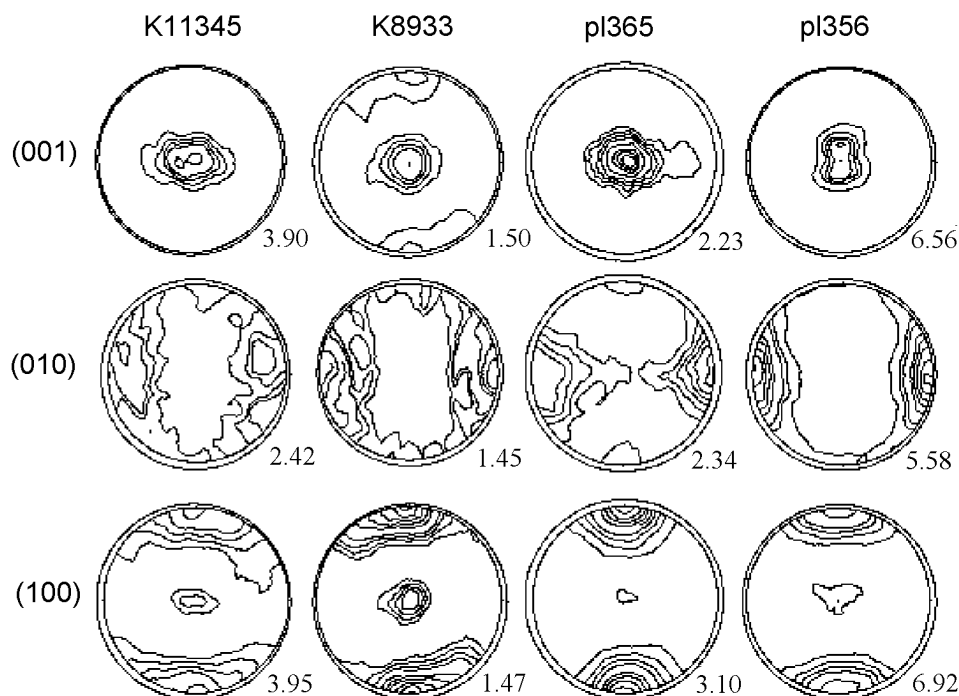


Figure 13. Hornblende pole figures of amphibolite samples calculated on the ODF basis. K11345, K8933 – samples from the Kola superdeep borehole; pl365, pl356 – samples from the surface of Mustantunturi area. The maximum values of the pole density in the units multiple of random distribution are indicated in the bottom right.

Note: The samples taken from the depth and the surface (four gneisses and four amphibolites) exhibit identical mineral (Figure 1) and chemical composition and the mineral density. Four core samples represent typical lithologies of the Archean basement (K11345, K8933 – amphibolites; K9002, K8658 – gneisses) of the borehole SG-3. The sample numbers indicate the depth of sample recovery in meters. Four samples (pl365, pl356 – amphibolites; pl363, pl358 – gneisses) from surface outcrops stand for the Archean basement. They were selected from the Mustantunturi site at a distance of 45 km northeast of the borehole because of similarities of geological structures.

metamorphic changes in the rock under influence of the changing pressure and temperature parameters could transform greatly the plagioclase texture without any destruction and having retained “memory” about the original stage of texture formation as identical orientation patterns on the (001) pole figures.

A mutual orientation of different mineral phases in the rocks different by the mineral composition might also, evidently, influence upon the progress of the mineral texture transformation. The interaction of the plagioclase with the hornblende, which is the main amphibolite rock-forming mineral and which retained a strong preferred orientation, has resulted in violation and even destruction of the original orientation much greater in amphibolites (Figure 14) than in gneisses (Figure 15) and this reflects on the (001) pole figures. The fact that the plagioclase pole figures have no pronounced regular orientations may also indicate to a strong recrystallization processes which have taken place during evolution of the Archean amphibolite rocks, that had more influence on the plagioclase than on the hornblende.

As there is a wide variety of the quartz textures, both in amphibolites and in gneisses (Figure 16), it is very dif-

ficult to interpret the mechanisms and conditions of their generation. Nevertheless, the texture analysis of quartz as a mineral component of the multiphase rock, has a lot of supplementary information regarding nature of the metamorphic processes, which influence upon evolution of the rock under investigation. There is a notion that the first (axial) type of the quartz texture observed on the PF may be formed during the plastic deformation under a plane strain deformation conditions, and the second type of orientation (unimodal) indicates to its formation by the simple shear.

A wide variety of the quartz textures, occupying an insignificant volume in the amphibolite samples, may be a result of a great diversity of the genetic processes in quartz, its polymorphism, a greater yielding to various metamorphic mechanisms. The latter transform the “relic” textures of quartz which appeared at the stage of generation of the amphibolite rock in the way that they can completely or partially be overlapped by a latter texture or, on the contrary, can be eroded during the cooling of the rock as a result of the phase transition and different types of twinning.

The following facts were brought to light as a result of investigation of an elastic anisotropy of the amphibolite spher-

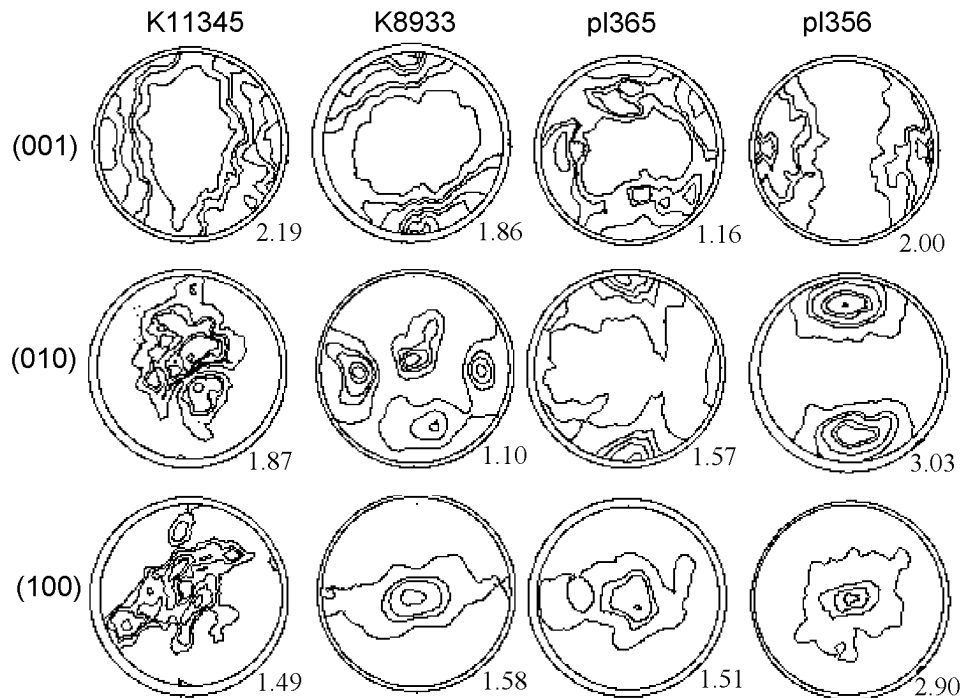


Figure 14. Plagioclase pole figures of amphibolite samples calculated on the ODF basis. K11345, K8933 – samples from the Kola superdeep borehole; p1365, p1356 – samples from the surface of Mustantunturi area. The maximum values of the pole density in the units multiple of random distribution are indicated in the bottom right.

ical samples at high hydrostatic pressures with the use ultrasonic sounding [Nikitin *et al.*, 2001b]. The anisotropy factor falls down in the pressure range of 0.1 up to 400 MPa for different samples from 2 to 6 times. This fact can be explained by a disintegration of the rock due to a decompression and a sharp cooling of the sample taken to the surface. The elastic wave velocity distribution throughout the range of pressures that reflect the nature of anisotropy, do not change practically and are caused by the hornblende texture. Taking into consideration the fact found earlier that the crystallographic textures of the hornblende of amphibolites taken from different depth and from the surface are practically identical, it is possible to state that the hornblende texture assigns a space-time coordinate system of the crust of the given geological region that remains unchanged for a long geological period. This creates conditions for application of the method of reconstruction of the paleotectonic stress/strain state from data on textures and seismic anisotropy of the amphibolite-containing blocks.

3.2. Reconstruction of Paleotectonic Stresses of the Ultrabasic Blocks from Data on Textures of Rocks and Seismic Anisotropy

It is known now, that majority of ultrabasic rocks belong to a spinel abyssal facies and do not show significant difference in chemical composition [Genshaft, 1974; Genshaft *et al.*, 1978; Grachev and Dobrzhinetskaya, 1987; Lutz, 1974,

1975]. The xenolith ellipsoidal, elongated-angular and disk-shaped samples occur, as a rule, on the surface [Grachev *et al.*, 1985]. The maximum size of xenoliths (over a long axis) reach sometimes 70 cm [Grachev and Dobrzhinetskaya, 1987; Grachev *et al.*, 1985].

It is well known from the laboratory experiments conducted by different authors on deforming the olivine polycrystals at different temperatures and pressures, that the texture formation takes place within the temperature range of (600–900°C), (900–1300°C), (1300–1600°C) by different slip systems. Comparison of the PF of the “reference” samples with the PF measured on the samples under investigation, permits to assess the depth where the deformation and texture formation processes were taken place and to appraise the thermodynamic parameters at the relevant depths from data of the neutron diffraction texture analysis. Experiments of different authors have shown that that the magmatic melt, which carries the xenoliths upwards, does not exert any significant influence upon their internal structure and texture [Dal Negro *et al.*, 1984; Eales and March, 1983; Fodor *et al.*, 1977; Grachev and Dobrzhinetskaya, 1987; Grachev *et al.*, 1985]. Many researchers adhere to a position that the external shape of xenoliths is predetermined by the tectonic processes in the upper mantle and the texture type is predetermined by the acted stress fields [Drubetskoi and Grachev, 1987; Kiselev *et al.*, 1987; Polyakov, 1987].

Importance of this information lies in the fact that it gives grounds to use a complex of experimental data obtained as a result of the neutron diffraction texture analysis and an

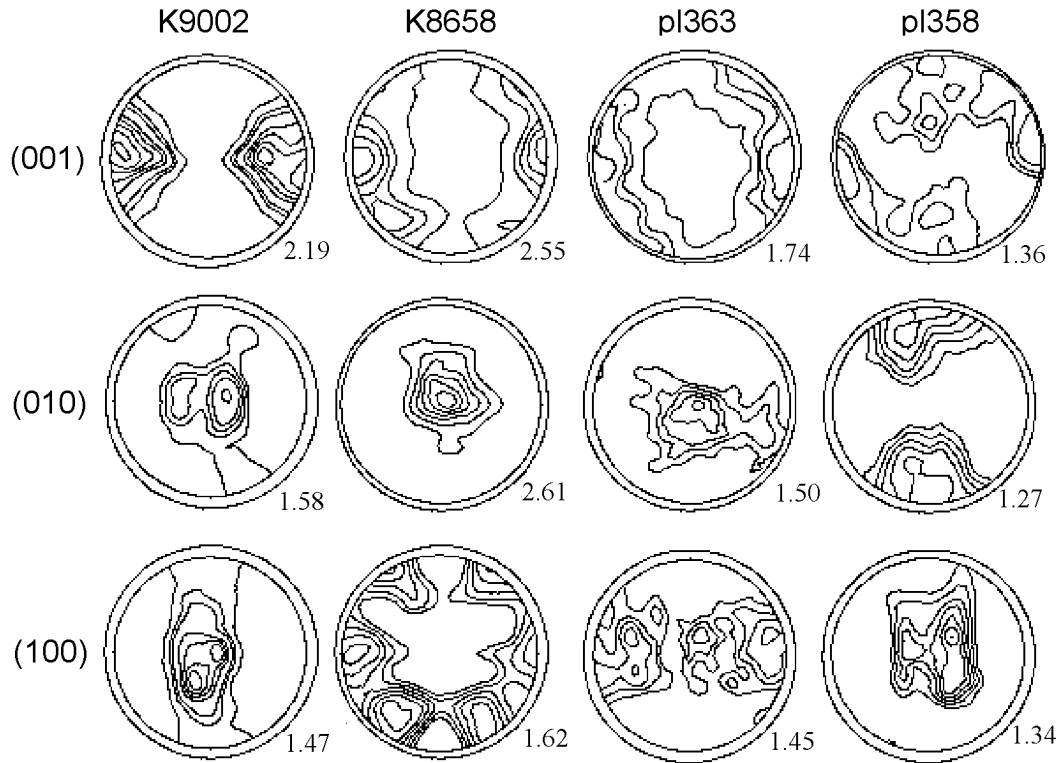


Figure 15. Plagioclase pole figures of gneiss samples calculated on the ODF basis. K9002, K8658 – samples from the Kola super deep bore hole; p1363, p1358 – samples from the surface of Mustantunturi area. The maximum values of the pole density in the units multiple of random distribution are indicated in the bottom right.

ultrasonic spatial detection determination of the maximum and minimum velocity of the longitudinal elastic waves to reconstruct a paleotectonic stress/strain state of blocks of the Earth's lithosphere. The experimental data on the relation of the olivine crystallographic textures and mechanical stress tensor, obtained from the laboratory deformation of the olivine samples at high pressures and temperatures and

from the analysis of the grain orientations and of the external forms of xenoliths, can be put into the basis of the reconstruction.

It has been found that the [001] main crystallographic axes of the deformed olivines are oriented as a rule, parallel to elongation of xenoliths. [010] axes are oriented parallel to the maximum compression. Arrangement of [100] axes has

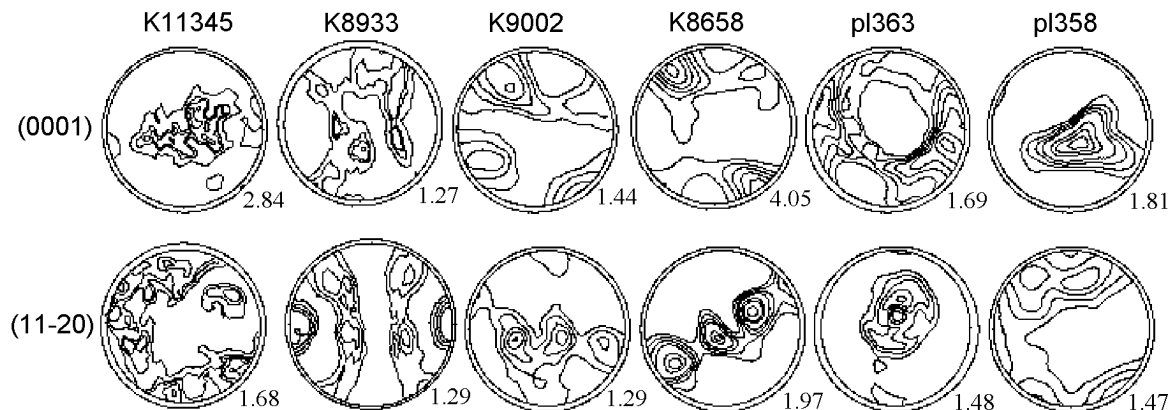


Figure 16. Quartz pole figures of amphibolite samples (K11345, K8933) and gneisses (K9002, K8658, p1363, p1358) calculated on the ODF basis. The maximum values of the pole density in the units multiple of random distribution are indicated in the bottom right.

a general tendency to be oriented parallel to the axis of the maximum xenolith extension.

It is well known the results of experiments on deformation of the synthetic dunite samples under the uniaxial compression at 1250–1300°C and at 130–140 MPa pressure of [Nikolas *et al.*, 1973]. At the same time, the preferred orientation of olivine is so, that [010] is also oriented along the axis of compression and axes [100] and [001] are oriented in the plane perpendicular to compression axis.

It has been found from a large series of samples [Nikitin *et al.*, 2001a], that the coordinate system of the pole figures, measured by neutron diffraction, is connected with the coordinate system of the elastic tensor (with the direction of the maximum and minimum velocity of the elastic waves) of the sample. This means, that directions of principle axis of the strain tensor can be found in the coordinate system of the elastic tensor of the anisotropic sample as is shown in Figure 17.

Likewise the amphibolites, which outcropped from lower levels of the crust, whose the relic texture of the hornblende is retained and it controls the elastic anisotropy of amphibolites, it becomes evident, that the type of olivines texture practically did not change in the dunites which had exhumated from the mantle. Consequently, the seismic anisotropy of blocks has also underwent some insignificant changes. This permits to use an up-to-date DSS in a complex with a complete texture analysis of the outcropped olivine-bearing dunites.

Thus, the reconstruction of the paleotectonic stressed-strain state in the lithosphere block which contains dunites presumes as follows:

1. Assessment of depths of samples of the olivine-bearing rock, which outcropped in different regions, by a complex of methods, the neutron texture analysis included.
2. Dating of samples.
3. Directional determination of the main axes of the elastic tensor on the spherical samples using of ultrasonic sounding.
4. Determination of the spatial orientation of the sample on the basis of data of the laboratory ultrasonic measurements and of the orientation of the main vectors of the seismic waves in the amphibolite or dunite block which is established by the deep seismic sounding (DSS).
5. Establishing orientation of the main axes of the strain (or stress) tensor in the coordinate system of the tensor of the elastic properties of the sample using of the texture data obtained by the neutron diffractometry.

3.3. Reconstruction of Orientation of Main Axes of Strain/Stress Tensor Based on Modeling the Texture Formation

The relation between types of the crystallographic textures of rocks and type of the mechanical stress tensor has been investigated experimentally [Kern, 1977] and theoretically [Nikitin and Ivankina, 1986; Sobolev and Demin, 1980].

The works mentioned above became a basis for the method of reconstruction of the paleotectonic stress-strain state in blocks of lithosphere, which influenced upon the texture for-

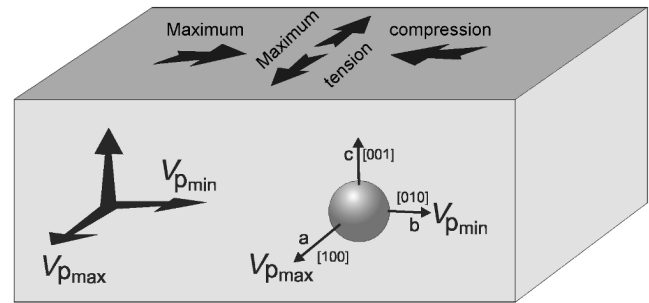


Figure 17. Example of the reconstruction of the stress/strain state of the Earth's lithosphere block.

mation of the quartz-bearing rocks, and afterwards texture was preserved [Nikitin *et al.*, 1991].

The modified Taylor model, which permits to obtain the pole figures in the coordinate system of the principal axes of the strain tensor for the given material, has been used as the basis for modeling of texture formation.

To texture formation simulation [Kurtasov, 1993] the following deformation conditions should be specified: temperature, strain-rate tensor components, the resulting strain and number of crystallites on the basis of which the model ODF will be restored; parameters of material should be also specified: slip systems, their critical shear stresses, activation energy, symmetry of the crystalline lattice.

Let us consider an example of modeling the texture formation in the quartz polycrystalline material, which deforms at a temperature exceeding $\alpha - \beta$ transition in quartz.

The action of the slip systems $(0001) \langle 1\bar{1}20 \rangle$ and $\{1\bar{1}01\} \langle 1\bar{1}20 \rangle$ (basic and pyramidal sliding planes) was taken into consideration in modeling of the high-temperature deformation of quartz. Aside of the above, a considerable number of other slip systems is also observed in quartz. It was supposed that the critical shear stresses at high temperatures (over 500°C) in these systems exceeds considerably the critical shear stresses in the easy slip systems.

Modeling of the axial compression in quartz gives an axial texture with a maximum near the axis of compression on the (0001) pole figure. The crystallographic directions lying in the base plane tend to turn towards the tension direction. The sharpness of the basis texture increases monotonously with the increasing of deformation degree.

The texture simulation at a pure shear was studied for the deformation 10^{-6} 1/sec rate, and in this case the deformation was modeled for a group consisting of 800 crystallites with the initial random orientations.

At a low and medium deformation degree an intermediate texture is formed, the (0001) poles turn to the plane perpendicular to the axis of elongation and (1010) poles of the planes turn to the axis of elongation. With further deformation the basic plane poles turn to the axis of compression and $(1\bar{0}10)$ poles continue to rotate to the axis of elongation. A single-component texture $(0001) \langle 1\bar{0}10 \rangle$ with a distinctive hexagonal symmetry of the pole figures.

To cite an example of reconstruction of the paleodeformation for sets of the veined quartz samples taken from one

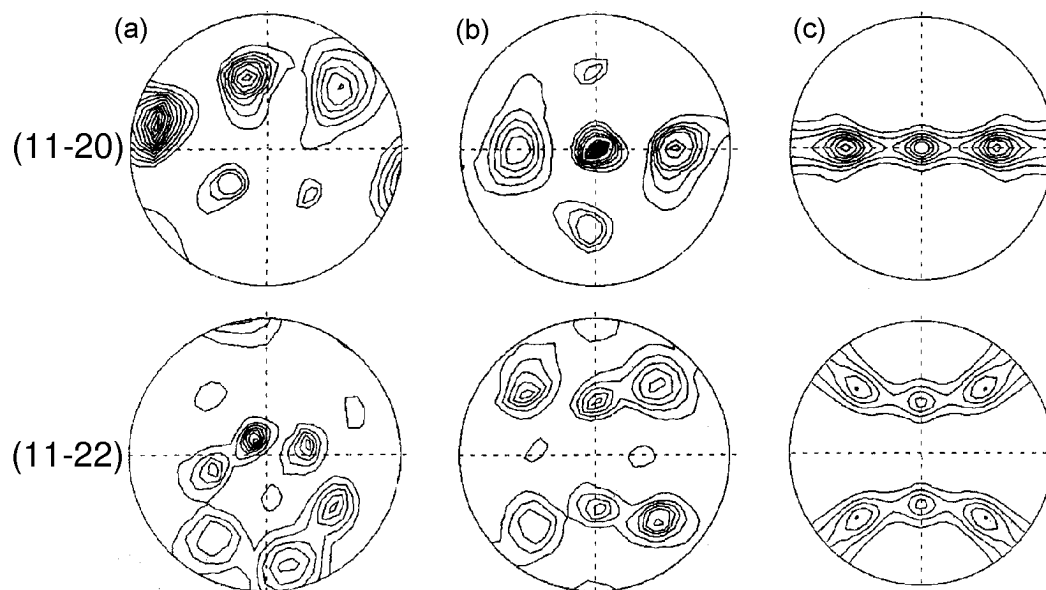


Figure 18. Veined quartz texture: a – experimental pole figures in respect to the laboratory coordinate system, b – after transformation into the probable principle axes of the strain tensor, c – model pole figures for pure shear.

of the quartz-ore gold deposits. The samples were taken orientally with respect to geological references. This permitted to bring the coordinate systems of the pole figures into agreement with the coordinate system of the sampling points.

The pole figures of both sets of samples were measured on the diffractometer NSHR (Dubna, Russia). Figure 18a shows two of the nine experimentally measured PF (11-20) and (11-22). The pole figures have no belts which are common for the texture at the axial deformation. This means that all the principal deformations of the sample differ and symmetry of the pole figures in the principal axes of the stationary deformation must be rhombic. Consequently, one transformation must symmetrize all the pole figures obtained.

Figure 18b shows the pole figures after rotation, which minimizes deviation of the pole figure symmetry from the orthorhombic one. The high sharpness of peaks on the pole figures can be explained by the fact that the rock was subjected to a great plastic strain. The additional X-ray investigations of the crystalline structure of two samples from the selected set have indicated to presence of slipbands and this indicates to a considerable plastic strain. There were no traces of recrystallization.

Thus, from consideration of symmetry, it is possible to determine the directions of the principal axes of strain. To determine relative values of the principal strain the experimental data must be compared with results of the computer simulation. Figure 18c shows the pole figures obtained by the pure shear simulation at 600°C and deformation 10^{-10} 1/sec rate. The best comparison of the model with experiment is ensured just at these parameters. A vertical direction on a stereographic projection corresponds to the principle tensile

deformation; there is no deformation in the horizontal direction and the compression component acts perpendicularly to the projection plain. The similar position of the pole density maxima on the experimental and simulation pole figures can be noted. A quality similarity of the experimental data with the simulation data permit to interpret the paleodeformation of two samples of veined quartz as a pure shear deformation.

The conditions found correspond to the plastic flow of quartz in the solid-phase hexagonal modification through the channel of a narrow crack. Thus, interpretation of the experimental data of neutron diffraction textures analysis of the oriented samples by computer simulation of the plastic deformation permits to reconstruct the paleodeformation scheme of the rock.

IV. Earthquake Source Theory and Neutron Investigations of Microstrains, Microstresses, Polymorphous Transformations in Minerals and Rocks in a Wide Range of Temperatures and Pressures

4.1. Neutron Diffraction Investigations of the Local and Residual Strains and Stresses of Rocks

Arrangement of extensive studies on the earthquake prediction required for a more deep knowledge of the physics of the earthquake preparation. Therefore, the laboratory experiments on the physics of materials fracture considering

the bedding conditions and specific properties of the rocks have been considerably expanded in many research centres. A special attention was paid to processes of the microcrack and macrocrack formation at the shear fracture and to the accompanying physical and mechanical changes of properties of the materials.

Advances in the physics of fracture, and especially, a purposeful seismological laboratory experiment permit even now to explain the field work results and open up new possibilities of forecasting studies. The level of the theory of fracture formation and concept on the seismic source, up-to-date laboratory experiments and the field observations, as a whole, permit to develop the theory of the earthquake preparation [Kasahara, 1985; Rais, 1982].

To understand the physics of fracture formation of such heterogeneous and anisotropic materials as rocks, it is necessary to consider the regularity of cracking, starting from the mineral crystalline lattices and breaking of the atomic bonding in the grain-boundary material [Sobolev *et al.*, 2001].

Application of the neutron scattering permits to measure intracrystalline strains and stresses in the local volumes and to investigate a strain-stress state within the sample in three dimensions. The following most important features of the neutron diffraction method should be noted:

1. A great depth of scanning the material (up to 2–3 cm for steel and up to 10 cm for aluminium).
2. A high spatial resolution (up to 1–2 mm in any measuring-in).
3. Using time-of-flight method allows to determine the crystallographic anisotropy of the intracrystalline mechanical deformations simultaneously (for different (hkl) planes) and to determine, by this way, anisotropy of the elastic and strength properties of the material.
4. In case of a multiphase material (composites, ceramics, rocks) neutrons present information about distribution of stresses for each phase separately.
5. Usually the deformation corresponding to the internal stresses is of the order of $\Delta d/d \times 10^{-3} - 10^{-4}$, therefore, a high resolution diffractometer is to be used for their measurement. The shift of the Bragg peak permits to determine strain lattice by an averaged measured volume. The information about microstresses (within one grain or several grains) can be obtained from broadening of the diffraction peaks.

Advantages of the neutron diffraction method are so important that special diffractometers were constructed in many up-to-date neutron centers in the last decade for the studying the intracrystalline stresses both on the steady-state reactors in Grenoble, Rzez and Berlin, and at the pulse neutron sources ISIS (Didcot, Chilton) and IBR-2 (Dubna).

Measurements of the intracrystalline stresses are based on determination of distance d between the atomic planes of the crystalline lattice of the material under investigation by a position of the relevant Bragg peak on the spectrum. Deformation of the lattice under stress leads to shifting of the peak. The relative value of the shift (relative strain) $\varepsilon = (d - d_0)/d_0$, where d_0 – interplanar spacing in the sample without internal mechanical stresses, characterizes the macroscopic lattice strain in the direction of the neutron scattering vector \mathbf{Q} which is perpendicular to the (hkl) plane.

The diffractometer EPSILON, intended for investigation of the local intracrystalline strain and stresses has been functioning on the channel 7A of IBR-2 since 1997 in the Frank LNP JINR (Dubna, Russia). A good spectral resolution is attained on the spectrometer due to a long time-of-flight path (about 102 m). The EPSILON has two narrow diaphragm detectors, which are arranged on opposite sides of the sample in the line perpendicular to the incident neutron beam.

The incident beam is scattered on the interplanar bases of crystallites with the Miller indices (hkl) (in this case the Bragg law is to be fulfilled). Then, the beam arrive at the detectors where the neutron diffraction spectra are recorded.

The EPSILON neutron diffractometer has a miniature pressure device machine EXSTRESS for loading of the cylindrical samples in the range of 1 up to 100 kN. Thus, the EPSILON can be used for measuring the residual deformations in the non-loaded samples and local intracrystalline strain inside the sample at different uniaxial external loads (0.1 up to 1000 MPa).

Operation of the EPSILON diffractometer was tested on a cylindrical sample of the Cretaceous sandstone, which was pressed through a steel tube for 20 hours after it had been extracted; this allowed to investigate the deformed and relaxed parts one the same [Scheffzük *et al.*, 1998]. For two mutually perpendicular radial directions of the cylinder the lattice spacing are much smaller in the gripped volume than in the free volume. Despite the results are not interpreted finally, influence and importance of the texture in strain-stress behavior of rocks is obvious.

At present the EPSILON diffractometer is being updated. The purpose of this is optimization of the neutron diffraction measurements to get a complete strain tensor. The updated Epsilon-MDS [Walther *et al.*, 2001] comprises nine detectors arranged in a circle with the angle of scattering for all the detectors is $2\Theta = 90^\circ$. This means that all the Bragg reflections are arranged in a similar position on the diffraction patterns from each detector and this is an advantage of the new detector system. In this case a better spectral resolution of 3×10^{-3} is attained. The lattice strain in the diffraction experiment is measured in the direction of the scattering vector, which coincides with the bisector of angle between the incident and scattered neutron beams. By specifying this direction the polar coordinates Φ and Ψ , one obtains an expression for the strain being measured

$$\begin{aligned} \varepsilon_{\Phi\Psi} &= (d_{\Phi\Psi} - d_0)/d_0 = \\ &= \varepsilon_{11} \cos^2 \Phi \sin^2 \Psi + \varepsilon_{12} \sin^2 \Phi \sin^2 \Psi + \\ &+ \varepsilon_{22} \sin^2 \Phi \sin^2 \Psi + \varepsilon_{33} \sin^2 \Psi - \varepsilon_{33} + \\ &+ \varepsilon_{13} \cos \Phi \sin^2 \Psi + \varepsilon_{23} \sin \Phi \sin^2 \Psi . \end{aligned} \quad (17)$$

This equation contains six unknowns. Measuring $d_{\Phi\Psi}$ for more than in six directions (with respect to coordinate system of the sample), it is possible to determine the independent components of the strain tensor ε , by solving a system of linear equations.

Measurement of strains at the other reactors are made with the help of a biaxial powder diffractometer equipped

with large position-sensitive detectors and special sample environment. The diffractometer E3 at the BER-II reactor of the Hahn-Meitner Institute (Berlin) as well as a high-intensity variable resolution diffractometer 20 at ILL (Grenoble) belong to this type of instruments. These instruments are employed for analyzing the residual stresses in the constructional materials when the requirements in $\Delta d/d$ resolution are pronounced compared to the demand for the geological materials.

The best resolution can be obtained at the pulsed sources due to the time-of-flight method. The ENGIN instrument for strain scanning is installed at the ISIS (Great Britain) spallation source and it functions according to the time-of-flight technique. It is characterized by a $\pm 90^\circ$ detector system, radial collimation and by a possibility to measure the interplanar spacing from 0.4 Å up to 3.3 Å. The $\Delta d/d$ resolution is of about 0,7% on the 15 m time-of-flight path. The gauge dimensions are 0.5×25 mm with respect to the incident beam in both dimensions and 1.5 mm in the scattered beam. The uniaxial loading permits to reach ± 50 kN and it is mounted on a position stage. Though this instrument is treated as the instrument for the engineering investigations, it has been recently successfully used for the study of the polymineral rocks. Criteria for application of the instrument for investigation of the rocks may expand considerably due to improvement of the $\Delta d/d$ resolution and to strain accuracy at the new ENGIN-X beam line with a 50 m time-of-flight path which is under construction.

The strain partitioning between the phase components in the polycrystalline calcite + halite aggregates [Rinaldi *et al.*, 2001] was studied on the basis of in situ deformation experiments when the sample was subjected to different loads in the neutron beam with the use of the ENGIN equipment at ISIS. By determining variations in lattice parameters of each phase as a function of the applied load, an elastic strain of each phase was estimated and, consequently, its contribution into the total deformation. Measurements of calcite/halite have revealed that the limit of elasticity of halite is reached at the strain about of 3.50×10^{-4} , and that the elastic strain partitioning between two phases is quite simple due to yielding of halite. With the elastic strain of calcite being more than 5.50×10^{-4} the strain partitioning between two phases tends to homogenous elastic strain. Thus, the neutron diffraction strain measurements provide a possibility to study the elastic properties of phase components of polymineral materials and to determine a relative contribution of each phase into the strength properties of the rock.

4.2. Neutron Diffraction Investigation of the Rock Properties at High Temperatures and Under External Loads

Combination of the texture analysis and measurements of the residual and lattice strain in samples is the most promising direction in application of the neutron scattering for investigation of properties of the geological materials. Such measurements for solving the geophysical problems become all the more important if they are conducted at different (high) pressures, temperatures and external loads.

The authors [Ivankina *et al.*, 2000] show the first results of measurements of the calcite lattice strain the marble, which were conducted in JINR (Dubna, Russia). The experiment was made on a special facility CUC (chamber for uniaxial compression at high temperatures) [Ivankina *et al.*, 1998]. The CUC chamber is placed in the center of a mounting ring of the SKAT spectrometer so that the sample subjected to heating compressing could be “seen” by all the nineteen detectors of the diffractometer simultaneously. The measuring is now up to 650°C and it is governed by the piston material and by permissible parameters of the temperature piezotransducers which help to measure velocity of the ultrasonic longitudinal waves during the tests. A capability of changing temperature and loads (measurements of these parameters) on the sample directly in the neutron beam is an important feature of the design.

The neutron measurements of the lattice strain on the same marble sample under a uniaxial compression only and under a simultaneous action of the uniaxial compression and temperature have shown the quite different lattice strains and stresses [Ivankina *et al.*, 2001]. The experimental results demonstrated the influence of temperature on behavior of marble under load and a principal importance of special thermoelastic properties of calcite.

The diffraction spectrum of marble was measured at the EPSILON at a room temperature without load and then the diffraction spectra were measured in succession under external stresses of 25 MPa, 32 MPa and 77 MPa without heating the sample. The external load increasing caused the peak shift on the spectra. To direct compression in the sample, the lattice strain of the interplanar spacing (11–23), (10–14), (21–31) were measured and on this basis the lattice stresses were calculated on assumption that deformation under all external loads obeys the Hooke’s law.

The same marble sample was used for measurements of the lattice strain at the simultaneous effects of temperature and mechanical load at the experimental complex SKAR-TKOS. This experiment is described in detail in the paper [Ivankina *et al.*, 2001].

The time-of-flight neutron diffraction spectra were recorded at different loads and temperatures; the relative deformations of the interplanar spacing of the crystalline lattices and thermal expansion coefficients were also determined. Forces on the pistons were measured along with recording of the diffraction spectra at the same temperatures. The macrostresses which increased as a result of thermal expansion of the sample was determined on the basis of the calibration dependence. The lattice stresses have been calculated for those temperatures at which the same external stresses were determined at the EPSILON (without heating).

Figure 19 shows the lattice stressed σ_{lattice} in the marble sample versus external compression load σ_{macro} curves, calculated at temperatures of 120°C, 220°C and at a room temperature for three crystallographic directions (11–23), (10–14) and (21–31).

The lattice stresses calculated for three external compression stresses –25, –32 and –77 MPa at a room temperature differ between each other depending on the crystallographic direction and in all cases they are less than the external

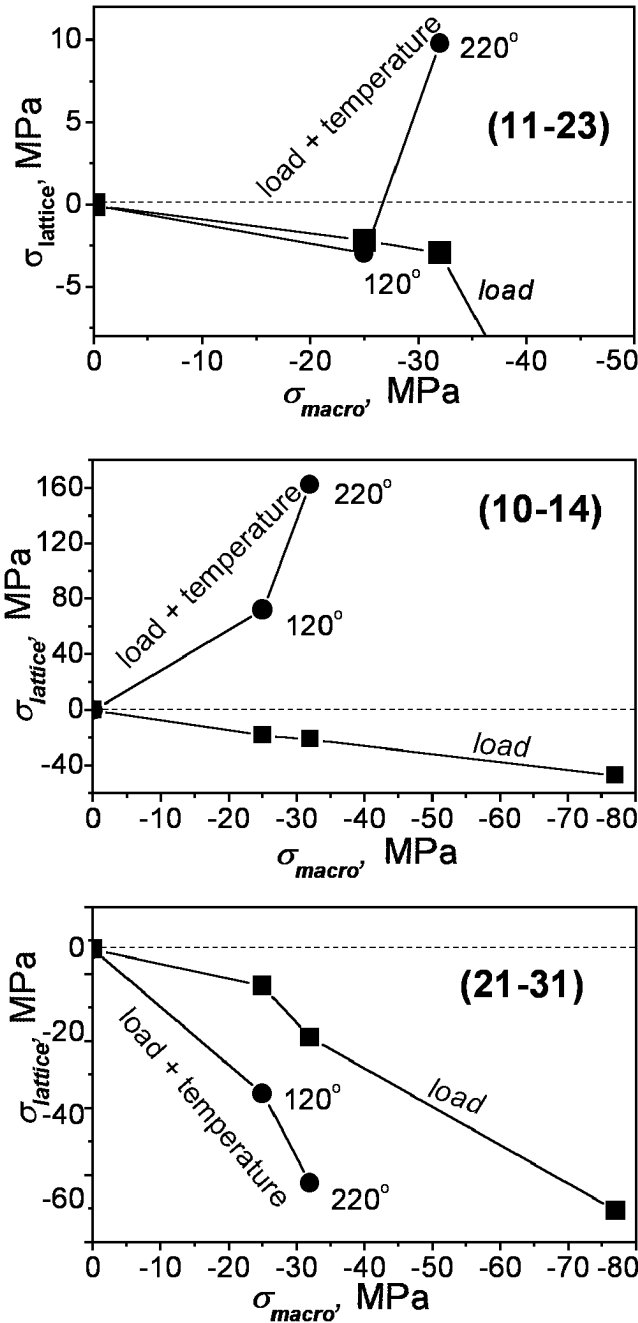


Figure 19. Dependence of the lattice stresses σ_{lattice} on the macroscopic stresses σ_{macro} : compression at lattice stresses at room temperature are marked by squares; lattice stresses of different signs, which occur at mechanical load and increased temperatures are marked by circles.

stresses applied to the sample. This can be explained by the fact that marble is a porous rock and that at small loads the deformation of material is composed of the linear crystalline

component of the sample and of the nonlinear component of the porous space.

At a simultaneous action of the mechanical load and temperature the picture is quite different. The lattice stresses for the same crystallographic directions (11–23), (10–14), (21–31) differ greatly and they exceed considerably the stresses applied to the sample. This difference increases with the temperature rise [Ivankina *et al.*, 2001].

From comparison of results of the two experiments (Figure 19) one can see that the lattice stresses depend on the crystallographic directions: they take maximum values in the (10–14) direction, middle values in the (21–31) direction and minimum values in the (11–23) direction.

The lattice stress in the (10–14) lattice direction at a temperature of 220°C and at the compression stress –32 MPa reaches the value of 162.4 MPa, that is comparable with the compressive strength of marble (the ultimate compression strength σ_c for different marbles is in the range of 180 to 300 MPa). The stress σ_{lattice} in the (11–23) direction changes its sign at 220°C with the increasing of the compression load and temperature and in the (10–14) direction sign change of lattice stress occurs at a much lower temperature of 120°C. This means that crystallites in these lattice directions deform by tension and not by compression, beginning from the above indicated temperatures.

The change of sign of the lattice stresses at a continuous increasing of the external compression and temperature can be explained by different signs of components of the thermal expansion tensor. At a simultaneous effect of the mechanical load, which deforms the sample by compression, and increasing temperature the role of the latter dominates. This means that deformation with a “plus” sign for some crystallographic directions is dictated by thermal expansion. As may be seen from the experiment, the tensile deformation opposing to the external compression develops in crystallites.

Stresses capable of initiating development of microcracking must correspond to great strains of crystallites, which are constrained inside the sample.

Reasons and conditions under which development of great local and lattice stresses in the rock (marble) were discussed in the paper by [Sobolev and Nikitin, 2001]. Because there are no rocks without destruction as shown in these tests, it can be assumed that those great lattice stresses, which were calculated on the basis of the measured microstrains inside the material. In our case great lattice strains did not cause the stresses which were calculated according to the Hooke’s law because of a considerable concentration of pores. The texture did not play a decisive role here because the neutron diffraction texture analysis of the sample has revealed a very weak texture.

The physical properties of the heterogenous, texturized, polycrystalline materials, which the rocks belong to, become apparent in different ways of the macro and micro scale levels. Consequently, the lattice stresses, calculated from strains measured by the neutron diffraction have reached the compression strength but the sample did not show any cracking after the test was completed.

4.3. Neutron Diffraction Investigation of Structure and Polymorphic Transformations in Minerals and Ice

In most cases neutron diffraction investigation is used as a for more precisely determining and obtaining supplementary data about structures which were previously examined by X-rays. Frequently the investigation is carried out with X-ray analysis in parallel and thus, information about cell, symmetry and arrangement of majority of atoms are already available. Capability of neutrons to penetrate deeply into the substance permits to investigate the crystalline structure at different temperatures, pressures and other external actions which along with the high resolution of the neutron flux give opportunities to the researchers that were not available earlier. A great advantage of the neutron diffraction investigation over X-ray analysis is more precise determination position of the light atoms in the presence of the heavy atoms.

Another advantage of the neutron diffraction investigation is the possibility to investigate structures containing atoms with close atomic numbers which are almost indistinguishable by X-ray. Compounds with Ni, Fe, Co etc. may serve as an example. Amplitudes of scattering b for such atoms or any isotopes differ widely to determine individual positions of these atoms. Difference in b for isotopes of the given element permits to state the problems on investigation of distribution and ordering of the isotope nuclei in crystalline structures.

Neutron diffraction has an explicit advantage for determining the crystallographic structures and transient processes in single crystals placed in various chambers. The peculiarities of interaction of neutrons with the substance determines a typical round of experiments on single crystals [Artioli, 2002]: determination of position of light atoms and geometry of hydrogen bonding (silica-alumina zeolites); investigation of cations partitioning between the crystallographic positions in minerals (albite, natrolite), what is important for understanding the physics and chemistry of the mineral generation.

Several examples of neutron investigations of the mineral and polymorphic formations at different pressures and at high and low temperatures can be cited [Dove, 2002]. The work of [Keen and Dove, 1998], conducted at ISIS neutron source on observation of structure of the silicate polymorphous states HP-tridymite, β -crystobolite, α -crystobolite, β -quartz, α -quartz at different temperatures can be related to this type of investigations. The temperature and pressure influence on the structural changes, on the order-disorder phase transitions, in particular, is studied by powder diffraction [Pavese, 2002]. The experiment on calcite [Dove and Powell, 1989] is this type of example, when order-disorder transition at 1260 K, accompanied by change of space group from $R\bar{4}c$ into $R\bar{3}m$ was observed. The work by [Dove et al., 2000] is dedicated to study of crystobolite structure at high pressure, which, as it turned out, corresponded to a distorted structure of high-temperature cubic β -phase.

Of great interest are investigations conducted by a team of the French scientists in the Laue-Langevin Institute

(Grenoble), early in the 80s [Berge et al., 1984; Dolino et al., 1983, 1984a, 1984b]. Results on the Bragg scattering of neutrons obtained in the work by [Dolino et al., 1983] conducted on a natural quartz sample of the D10 diffractometer. When quartz was cooled from the β -phase a weak increasing diffuse scattering was observed around the (301) Bragg's peak, and then at a temperature of $T(\beta \rightarrow \alpha) + 1.5$ K this scattering became anisotropic and two symmetric satellite peaks appeared, whose intensity was rising in a linear mode along with the change of temperature. Intensity of satellites increased sharply at a temperature of the phase transition $T(\beta \rightarrow \alpha)$ that corresponded to the II kind transition. In this case appearance of an intermediate phase in the temperature range 1.3 K over $T(\beta \rightarrow \alpha)$ was confirmed by a measurement of sample heat capacity. The accuracy of the neutron diffraction experiment, however, did not allow to state whether the satellite peaks appear exactly at a temperature of $T(\beta \rightarrow \alpha)$ or this is some other anomaly.

Subsequently the same authors fulfilled a more precise experiment (with stabilization temperature of 0.02 K), presented in the paper [Dolino et al., 1984b], which is included into a cycle of articles, where results obtained from the neutron elastic scattering method are compared with the results of the electron-microscopy investigation. The neutron measurements were made on a volume quartz sample (up to several cm^3) and were accompanied by a continuous measurements of thermal expansion. It was confirmed as a result of experiments that the $\alpha - \beta$ quartz transformation occurs with formation of an incommensurate phase, which exists in a small temperature range of 1 to 2 K. The β -quartz transition into the incommensurate phase is continuous, the incommensurate phase - α -quartz is the I kind transition. Noted was also an increasing of intensity of the diffuse scattering of neutrons near the phase transition point. This result is in agreement with the Landau theory regarding the crystals suffering the II kind phase transition.

An unusual behavior of α -quartz at high pressures has become an object of the experimental investigation [Kingma et al., 1993] with the use of a synchrotron X-ray diffraction. The test was conducted on the powder samples and on the natural quartz samples under a static compression. It has been found that with the increasing of pressure up to 21 GPa, a crystallite-crystallite metastable transition, which is observed during amorphisation in quartz. This transition was considered as an intermediate phase in amorphisation by analogy with the incommensurate phase at a high-temperature $\alpha - \beta$ transition in quartz.

Of interest are experiments on the study of the phase transitions in molecular hydrogen and methane for the physics of planets. Investigation of the molecular H_2 and of other molecular systems - H_2O , NH_3 , H_2S , CH_4 presents a great interest at superhigh pressures, when density of the substance is sufficiently high that the chemical bond-site can change in these system. It is assumed that at a very high pressures the molecular hydrogen H_2 transforms into a metallic state and H_2O ice changes into a simple oxide with the same length of the hydrogen bonds H-O. Currently much attention was paid to a search of this modification of ice. These compounds are the main components of the crust of other planets, of Uranus and Neptune especially.

Therefore, the structure investigations of these substances are important for understanding the change in interatomic relations at high densities of the substance and for the study of the structure and processes taking place on other planets.

The equation of the state of molecular deuterium D_2 was investigated at the DISC diffractometer on a steady-state reactor IR-8 (RSC KI, Moscow) at pressures up to 310 kbar. The experiments were made on the single crystalline samples with the use of magnetic anvils. At a compression D_2 remains in the initial lattice and is close to ideal and depends but slightly from pressure [Glazkov *et al.*, 1988]. The equation of state obtained differs rather greatly from of the theoretical calculations. This testifies that estimations given by theory for pressure at which metallization of hydrogen takes place are far from actual values.

At present 12 modifications of ice are known and its structure was thoroughly investigated at pressures up to 3 GPa [Whalley *et al.*, 1968]. However, information about the ice structure at higher pressures was coming from the neutron diffraction measurements of the O-O space changes [Hemley *et al.*, 1987] and the empirical relations between the change of O-O and O-H space obtained from investigation of different compounds at a normal pressure. The texture investigation of the substance of the Moon, consisting mainly of the rock and ice mixture, is needed to establish its planetary history. Understanding of behavior of ice at high pressures and low temperatures is essential for any kind of the geological or geophysical interpretation.

The texture of polycrystalline ice II high pressure (polymorph modification of solid form of water, which is stable approximately between 200 and 500 MPa and below 238 K, rhombohedral crystal structure), which was obtained in the low-temperature experiments at high pressure and uniaxial compression, was studied at temperature of 77 K [Bennett *et al.*, 1994]. The pole figures of two deuterated samples (one was synthesized at a hydrostatic pressure and was shortened to 50% at 225 K, the other was obtained without hydrostatic pressure and was shortened by 7% at 195 K), calculated on the ODF basis show that the a-axes align in the direction of compression. In the polymorphous modification of the low-pressure ice I, which was deformed at low temperature, c-axes are oriented parallel to the direction of compression [Kocks *et al.*, 1998]. It was proved by the experiments conducted at the ILL that texture in the sample of non-deuterated ice can be measured and the ODF restored, even at a strong incoherent scattering of H .

Conclusion

Many fundamental researches in various fields of geology and modern geophysics do not dispense now without application of neutron diffraction analysis to study of structure, texture and properties of geological materials as well as in simulation of the geodynamic effects especially at low and high temperatures and under hydrostatic and nonequaxial pressures.

The Russian scientists from the JINR collaborating with the scientific centers of Germany (Institute of geology and

dynamics of lithosphere of the Göttingen University, Center of geological investigations in Potsdam, Institute of the geological investigations of the Kristian-Albrecht University in Kiel) conduct systematic investigations in frames of a joint program.

A joint investigations of the physical nature of seismic anisotropy and on physics of the rocks fracturing are developing with the Geophysical Institute and with the Institute of the rock structure and mechanics of the Czech Academy of Sciences, the United Institute of physics of the Earth, RAS.

The number of neutron sources will be reduced early in this century as reactors whose service life has been depleted will be taken out of service. The IBR-2 reactor at the JINR will be in a long outage in 2007 because of its rehabilitation. Therefore, a productive application of neutron diffraction for solving the problems of geology and geophysics should be based on improvement of efficiency and information density of experiments which are to be selected and conducted for the most important fundamental and applied problems of the Earth's sciences.

The following may be place in the category of these problems:

- Classification of types of rock textures of the crust and upper mantle of the Earth with the purpose of clarifying knowledge about structure of lithosphere, nature of the seismic anisotropy and the geomechanical stability of the continental crust.
- Search of anomalous behavior the geological materials during the microstructure transformations under the changing thermal conditions and mechanical stress fields.
- Investigation of the phase transition kinetics in different minerals and rocks at high thermodynamic parameters.
- Study of changes in physical properties of rocks under temperatures, mechanical stresses and radioactive radiation as well as of regularities of interaction of shape textures and crystallographic textures, which influence upon directions of movement of fluids in the crust, with the aim of selecting optimum materials for construction of the radioactive and chemical wastes storages and for estimation of risk of storing the wastes at a great depth.
- Investigation of regularities of distribution of local stresses in the texturized rock in a wide range of temperatures and mechanical stresses from the point of view of the earthquake source theory.
- Ascertainment of regularities, physical mechanisms and a chronological sequence of the deformation and metamorphic processes in lithosphere from a complex of geophysical, geochemical and neutron diffraction data.

References

- Activation analysis of rocks and of other objects*, Collect. of articles, Fan, Tashkent, 1967.
- Adams, B. L., S. I. Wright, and K. Kunze, Orientation imaging: the emergence of a new microscope, *Metall. Trans.*, 24A, 819–831, 1993.
- Aksenov, V. L., Neutron physics on the threshold of the XXI century, *Physics of elementary particles and E1 (nuclei)*, 31, (issue 6) 1303–1342, 2000.
- Aleksandrov, K. S., and G. P. Prodaivoda, *Anisotropy of elastic properties of minerals and rocks*, 354 pp., Izd-vo Sib. Branch RAS, Novosibirsk, 2000.
- Artioli, G., Single-crystal neutron diffraction, *Eur. J. Mineral.*, 14, 233–239, 2002.
- Asanidze, B. Z., A. V. Lomidsze, and D. M. Pechersky, Spatial orientation of magnetic texture of volcanic lava in Kazbegi region, *Transactions of the international conference "Physical/chemical and petrophysical investigations in sciences about the Earth"*, pp. 7–8, Moscow, 2001.
- Babuska, V., and M. Cara, *Seismic anisotropy in the Earth*, 217 pp., Kluwer Academic Publishers Dordrecht/Boston/London, 1991.
- Barenblatt, G. I., et al., Kinetics of crack propagation, *Eng. mag., MTT*, part 1 and 2, no. 5–6, 1966.
- Bayuk, E. I., M. P. Volarovich, and F. M. Levitova, *Elastic anisotropy of rocks at high pressures*, 169 pp., Nauka, Moscow, 1982.
- Benn, K., and D. Mainprice, An interactive program for determination of plagioclase crystal axes orientations from the U-stage measurements: an aid for petrofabric studies, *Computers and Geosciences*, 12, 1127–1142, 1989.
- Bennett, K., H.-R. Wenk, C. S. Choi, S. F. Trevino, W. B. Durham, and L. A. Stern, Texture measurement at 77 K of deformed D₂O ice II polycrystals: a study by neutron diffraction, in *Textures of geological materials*, (edited by Bunge H.-J., Siegesmund S., Skrotski W. and Weber K.), pp. 251–260, DGM special publication, 1994.
- Bennett, K., R. B. von Dreele, and H.-R. Wenk, "HIPPO", a new high intensity neutron diffractometer for characterization of bulk materials, in *"Proc. ICOTOM-12"*, J. A. Szpunar, Ed., NRC Research Press, Ottawa, Canada, vol. 1, pp. 129–134, 1999.
- Berge, B., G. Dolino, et al., Incommensurate phase of quartz: II. Brillouin scattering studies, *J. Physique*, 45, 715–724, 1984.
- Bishop, J. R., Piezoelectric effects in quartz-rich rocks, *Tectonophysics*, 77, 297–321, 1981.
- Brokmeier, H.-G., U. Zink, R. Schnieber, and B. Witassek, TEX-2, Texture analysis at GFSS Research Center, *Mat. Sci. Forum*, 273–275, 277–282, 1998.
- Bukharova, T. I., and T. I. Savelova, Application of normal distribution on SO(3) and S² for orientation distribution function approximation, *Textures and Microstructures*, 21, 161–176, 1993.
- Bunge, H. J., Zur darsstellung allgemeiner texturen, *Z. Metallkunde*, 56, (2), 872–874, 1965.
- Bunge, H. J., Texture analysis in material science, *Mathematical methods*, 330 pp., Butterworth, London, 1982.
- Chateigner, D., H.-R. Wenk, and M. Pernet, Orientation distributions of low symmetry polyphase materials using neutron diffraction data: Application to a rock composed of quartz, biotite and feldspar, *Textures and Microstructures*, 33, 35–43, 1999.
- Chekin, B. S., Effective parameters of elastic medium with random distributed cracks, *Izvestia Acad. Sci. USSR, Fizika Zemli*, (4), 13–21, 1970.
- Cherepanov, G. P., Propagation of cracks in continuum, *PMN*, 31, (3), 1967.
- Dal Negro, A., S. Carbonin, C. Domeneghetti, G. M. Molin, A. Gundari, and E. M. Picciril, Crystal chemistry and evolution of the clinopyroxene in a suite of high-pressure ultramafic nodules from Newer Volcanics, Australia, *Contribs, Mineral. and Petrol*, 86, 221–229, 1984.
- De Wall, H., M. Bestmann, and K. Ullemeyer, Anisotropy of dia-
- magnetic susceptibility in Thassos marlbe: A comparison between measured and modelled data, *J. Struct. Gel.*, 22, 1761–1771, 2000.
- Dolino, G., J. P. Bachheimer, and C. M. E. Zeyen, Observation of an intermediate phase near the $\beta - \alpha$ transition of quartz by heat capacity and neutron scattering measurements, *Solid state comm.*, 45, (3), 295–299, 1983.
- Dolino, G., B. Berge, et al., Incommensurate phase of quartz: I, Elastic neutron scattering, *J. Physique*, 45, 361–371, 1984a.
- Dolino, G., J. P. Bachheimer, et al., Incommensurate phase of quartz: III, Study of the coexistence state between the incommensurate and the α -phases by neutron scattering and electron microscopy, *J. Physique*, 45, 901–912, 1984b.
- Dove, M. T., and B. M. Powell, Neutron diffraction study of the tricritical orientational order/disorder phase transition in calcite at 1260 K, *Phys. Chem. Minerals*, 16, 503–507, 1989.
- Dove, M. T., and M. S. Craig, Crystal structure of the high pressure monoclinic phase-II of cristobalite SiO₂, *Min. Mag.*, 64, 569–576, 2000.
- Dove, M. T., An introduction to the use of neutron scattering methods in mineral sciences, *Eur. J. Mineral.*, 14, 203–224, 2002.
- Drubetskoi, E. P., and A. F. Grachev, Basalts and ultrabasic xenoliths of the Baikal rift zone, *Isotopy of helium and argon. Deep xenoliths and lithosphere structure*, pp. 54–63, Nauka, Moscow, 1987.
- Eales, H. V., and J. S. March, Al/Cr ratios of coexisting pyroxenes and spinellides in some ultramafic rocks, *Chem. Geol.*, 38, 57–74, 1983.
- Fedorov, E. S., *Theodolite method in geology and in petrography*, 1893.
- Feldmann, K., M. Betzl, W. Kleinsteuber, and K. Walther, Neutron time-of-flight texture analysis, *Textures and Microstructures*, 14–18, 59–64, 1991.
- Flerov, G. N., Application of nuclear physics methods for exploration and development of the oil and gas fields, *Radioisotopes in the Physical Sciences and Industry, Press. Conf. Sept.*, Vol I, pp. 117–122, Vienna, IAEA, 1960.
- Fodor, R. V., K. Keil, and G. R. Bauer, Contributions to the mineral chemistry of Hawaiian rocks, V, Composition and origin of ultramafic nodules and megacrysts in a Rhyodacite from Oahu, Hawaiian Islands, *Pacif. Sci.*, 31, 211–222, 1977.
- Genshaft, Yu. S., *Experimental simulation of mineral composition of lowermost strata of crust and of upper mantle*, pp. 32–45, Nauka, Moscow, 1974.
- Genshaft, Yu. S., V. A. Ermakov, and A. Ya. Saltykovsky, Construction of regional physico-chemical models of underground processes and of the earth crust and upper mantle structure, *Izv. Acad. Sci. USSR, Fizika Zemli*, (9), 91–110, 1978.
- Ghildiyal, H., E. Jansen, and A. Kirfel, Volume texture of deformed quartzite observed with U-stage and neutron diffraction, *Textures and Microstructures*, 31, 239–248, 1999.
- Ghomshei, M. M., and T. L. Templeton, Piezoelectric and a-axes fabric along a quartz vein, *Phys. of the Earth and Planet. Int.*, 55, 374–386, 1989.
- Glazkov, V. P., S. P. Besedin, I. N. Goncharenko, A. V. Irodova, I. N. Makarenko, V. A. Somenkov, S. M. Stishov, and S. Sh. Shilshtein, *Letters to Zh. ET*, 47, 661, 1988.
- Grachev, A. F., V. V. Nikolaichik, and V. P. Trubytyn, About nature of regular form and ultrabasic xenoliths in basalts and regularities of their size distribution, *Dokl. Acad. Sci. USSR*, 285, (6), 1433–1435, 1985.
- Grachev, A. D., and L. F. Dobrzhinetskaya, *Structural anisotropy of the mantle xenoliths from neogenic vulcanites of the Central Europe and its importance for interpretation of the azimuthal seismic anisotropy of lithosphere. Deep xenoliths and lithosphere structure*, pp. 178–193, Nauka, Moscow, 1987.
- Griffith, *The theory of rupture*, Proc. I Internat. Congr. Appl. Mech. Delft, 1924.
- Hadley, K., Comparison of calculated and observed crack densities and seismic velocities of westerbi granite, *J. Geophys. Res.*, 81, (20), 3484–3494, 1976.
- Heilbronner, P., and C. Pauli, Interated spatial and orientation

- analysis of quartz c-axes by computer-aided microscopy, *J. Struct. Geol.*, **15**, 369–382, 1993.
- Helming, K., Method of geometric approximation for a texture analysis of rocks, *Fizika Zemli*, (3), 73–82, 1993.
- Helming, K., and T. Eschner, A new approach to texture analysis of multiphase materials using a texture component model, *Crystalline Research Technology*, **25**, K203–K208, 1990.
- Helming, K., A. N. Nikitin, and K. Walther, Neutron texture investigation of a meteor, *Textures and Microstructures*, **14–18**, 279–283, 1991.
- Hemley, R. J., A. P. Jephcoat, H. K. Mao, C. S. Zha, L. W. Finger, and D. E. Cox, *Nature*, **330**, 737, 1987.
- Hofler, S., G. Will, and H.-M. Hamm, Neutron diffraction pole figure measurements on iron meteorites, *Earth Planet. Sci. Lett.*, **90**, 1–10, 1988.
- Holt, D. B., M. D. Muir, P. R. Grant, and I. M. Boswarva, *Quantitative scanning electron microscopy*, Academic Press, New York, 1974.
- Honikomb, R., *Plastic deformation of metals*, 408 pp., Mir, Moscow, 1972.
- Hrouda, F., Magnetic anisotropy of rocks and its application in geology and geophysics, *Geophys. Surv.*, **5**, 37–82, 1982.
- Hrouda, F., H. Siemes, N. Herres, and C. Hehlig-Michaeli, The relationship between the magnetic anisotropy and the c-axis fabric in a massive hematite ore, *J. Geophys.*, **56**, 174–182, 1985.
- Hrouda, F., and K. Schulmann, Conversion of the magnetic susceptibility tensor into the orientation tensor in some rocks, *Physics of the Earth and Planetary Interiors*, **63**, 71–77, 1990.
- Jansen, E. M., H. Siemes, P. Merz, W. Schäfer, G. Will, and M. Dahms, Determination of preferred orientation of pyrite in a chalcopyrite ore by means of neutron diffraction, *Textures and Microstructures*, **19**, 203–210, 1992.
- Ivankina, T. I., A. N. Nikitin, W. Voitov, and K. Walther, Texture analysis and investigation of piezoelectric properties of natural quartz, *Textures and Microstructures*, **14–18**, 421–429, 1991.
- Ivankina, T. I., A. N. Nikitin, K. Ullemeyer, et al., Investigation of structure and texture transformation processes in rocks, *Schriften. f. Geowiss.*, (6), 49–56, 1998.
- Ivankina, T. I., A. N. Nikitin, T. Locajicek, Z. Pros, et al., Textures and elastic anisotropies of amphibolites from the Kola borehole, *Proceedings of the Twelfth International Conference on Textures of Materials*, vol. 2, pp. 1587–1592, Montreal, Canada, 1999a.
- Ivankina, T. I., K. Klima, T. Lokaichek, A. Nikitin, and Z. Pros, Investigation of anisotropy of the olivine xenolite with the help of acoustic waves and neutron diffraction, *Fizika Zemli*, (5), 29–39, 1999b.
- Ivankina, T. I., A. N. Nikitin, A. S. Telepnev, et al., Textures and physical properties of marbles deformed at 20–250°C, *High Pressure Research*, **17**, 335–346, 2000.
- Ivankina, T. I., A. N. Nikitin, A. S. Telepnev, K. Ullemeyer, G. A. Efimova, C. M. Kireenkova, G. A. Sobolev, V. A. Sukhoparov, and K. Walther, Influence of temperature and a long mechanical stress on deformation, thermal and texture characteristics of marble, *Fizika Zemli*, (1), 50–65, 2001.
- Kalinin, V. A., and I. O. Bayuk, Elastic anisotropy of the medium with oriented system of cracks with arbitrary shape and concentration, *Doklad RAS*, **338**, (3), 1994.
- Kachanov, A. N., About the crack growth kinetics, *PMN*, **25**, (iss. 3), 1961.
- Karato, S.-I., Seismic anisotropy due to lattice preferred orientation of minerals: Kinematic or dynamic? *High-Pressure Research in Mineral Physics*, pp. 455–471, Orlando, FL: Academic Press, 1987.
- Kasahara, K., *Earthquake mechanics*, 263 pp., Mir, Moscow, 1985.
- Keen, D. A., and M. T. Dove, Local Structures of silica polymorphs, *The Rutherford Appleton Laboratory ISIS Facility Annual Report 1997–1998*, pp. 44–45, 1998.
- Kern, H., Preferred orientation of experimentally deformed limestone marble, quartzite and rock salt at different temperatures and states of stress, *Tectonophysics*, **39**, (1–3), 103–120, 1977.
- Kingma, K. J., R. J. Hemley, Ho-kwang Mao, and D. R. Veblen, New high-pressure transformation in α -quartz, *Phys. Review Lett.*, **70**, (25), 3927–3930, 1993.
- Kiselev, A. I., V. G. Semenova, L. V. Solov'eva, S. V. Rasskazov, and B. M. Vladimirov, Deep xenolites in basalts of the Baikal rift zone and Tokin stanovik, *Deep xenolites and lithosphere structure*, pp. 64–72, Nauka, Moscow, 1987.
- Kocks, U. F., C. N. Tomé, and H.-R. Wenk, *Texture and anisotropy*, Cambridge university press, 676 p., 1998.
- Kostrov, B. V., *Mechanics of the tectonic earthquake*, Nauka, Moscow, 1975.
- Kranz, R. I., Microcracks in Rocks, A. Review, *Tectonophysics*, **100**, (1–3), 449–480, 1983.
- Kruhl, J. H., Computer-assisted determination and presentation of crystallographic orientations of plagioclase on the basis of universal-stage measurements, *N. Jb. Miner. Abh.*, **157**, 185–206, 1987.
- Kurtasov, S. F., Procedure of simulation of deformation textures, *Factory laboratory*, **59**, (11), 31–34, 1993.
- Leiss, B., and T. Weiss, Fabric anisotropy and its influence on physical weathering of different types of Carrara marbles, *Journal of Structural Geology*, **22**, 1737–1745, 2000.
- Lloyd, G. E., An appreciation of the SEM electron channeling technique for petrofabric and microstructural analysis of geological materials, in *Textures of geological materials* (edited by Bunge H.-J., Siegesmund S., Skrotzki W. and Weber K.), pp. 93–126, DGM special publication, 1994.
- Locajicek, T., Z. Pros, K. Klima, et al., Laboratory investigation of elastic anisotropy and texture of rocks from Kola Super Deep Borehole SG-3, International Conference “Textures and Physical Properties of Rocks”, *Gottinger arbeiten zur geologie und palaontologie*, Gottingen, vol. 2, p. 114, 1999.
- Lobanov, K. V., V. I. Kazansky, A. V. Kuznetsov, A. V. Zharikov, A. N. Nikitin, T. I. Ivankina, and N. V. Zamyatina, Comparison of the Archean rocks from the Kola super deep bore hole and their analogues from the surface by results of the structural-petrological, petrophysical and neutron diffraction investigations, *Petrologia*, (1), 30–45, 2002.
- Lutterotti, L., S. Matthies, H.-R. Wenk, et al., Combined texture and structure analysis of deformed limestone from time-of-flight neutron diffraction spectra, *J. Appl. Phys.*, **81**, 594–599, 1997.
- Lutz, B. G., *Petrology of deep zones of the continental crust and upper mantle*, 304 pp., Nauka, Moscow, 1974.
- Lutz, B. G., *Chemical composition of the continental crust and upper mantle of the Earth*, 167 pp., Nauka, Moscow, 1975.
- Mainprice, D., and A. Nicolas, Development of shape and lattice preferred orientations: application to the seismic anisotropy of the lower crust, *J. Struct. Geol.*, **11**, 175–189, 1989.
- Matthies, S., On the reproducibility of the orientation function of texture samples from pole figures (Ghost phenomena), *Phys. Stat. Sol. (b)*, **92**, K135–K137, 1979.
- Matthies, S., G. W. Vinel, and K. Helming, Standart distribution in texture analysis, *Berlin. Acad. Verlag*, vol. 1–3, 1987–1988, 1989.
- Neutron-activation analysis*, Coll. of articles, “Zinatne”, Riga, 1966.
- Nikitin, A. N., Formation of piezoelectric textures in quartz-bearing rocks, *Fizika Zemli*, (10), 15–21, 1996.
- Nikitin, A. N., *Anisotropy and textures of materials, Course of lectures*, Izd. MGUMGY, 260 pp., 2000.
- Nikitin, A. N., and I. K. Arkhipov, Simulation of texture formation in quartz-bearing rocks at phase transition temperature, *Fizika Zemli*, (12), 29–40, 1992.
- Nikitin, A. N., and T. I. Ivankina, About connection of piezoelectric textures of quartz with the stressed state type, *Izv. Acad. Sci. USSR, Fizika Zemli*, (3), 48–57, 1986.
- Nikitin, A. N., and T. I. Ivankina, On the possible mechanisms of the formation of piezoelectric active rocks with crystallographic textures, *Textures and Microstructures*, **25**, 33–43, 1995.
- Nikitin, A. N., and E. I. Parkhomenko, Piezoelectric textures of quartz-bearing rocks and their symmetric properties, *Izv. Acad. Sci. USSR, Fizika Zemli*, (2), 30–39, 1982.
- Nikitin, A. N., et al., Measurement of angular dependences of

- piezoeffect in piezoactive samples, *Izv. Acad. Sci. USSR, Fizika Zemli*, (12), 36–44, 1981.
- Nikitin, A. N., T. I. Ivankina, and A. B. Uspenskaya, About one method of reconstruction of peletotectonic stresses within the tectonic block, *DAS USSR*, 318, (1), 168–171, 1991.
- Nikitin, A. N., V. P. Pereygin, and D. E. Burylichev, Neutron diffraction investigation of damages in tracks of fast heavy nuclei in meteorites, *Izvestia, Tulgosuniversitet. Ser. Fizika*, Iss. 2, 3–17, 1999.
- Nikitin, A. N., T. I. Ivankina, D. E. Burylichev, K. Klima, T. Lokaichek, and Z. Pros, Anisotropy and texture of olivine-bearing mantle rocks at high pressures, *Fizika Zemli*, (1), 64–78, 2001a.
- Nikitin, A. N., T. I. Ivankina, K. Ullemeyer, et al., Texture controlled elastic anisotropy of amphibolites from the Kola superdeep borehole SG-3 at high pressure, *Fizika Zemli*, (1), 41–49, 2001b.
- Nicolas, A., F. Boudier, and A. M. Boullier, Mechanisms of flow in naturally and experimentally deformed peridotites, *Amer. J. Sci.*, 273, 853–876, 1973.
- Nikolayev, D. I., T. I. Savolova, and K. Feldman, Approximation of the orientation distribution of grains in polycrystalline samples by means of Gaussian, *Textures and Microstructures*, 19, 9–27, 1992.
- Nozik, Yu. Z., R. P. Ozerov, and K. Hennig, *Neutrons and a solid body, Structural neutronography*, Vol. 1, 343 pp., Atomizdat, Moscow, 1979.
- Nuclear geophysics*, Coll. of articles, 560 pp., Mir, Moscow, 1964.
- Ozerov, R. P., *History, development and trends of neutronography, Poverhnoct'*, (7), 8–19, 1997.
- Pavese, A., Neutron powder diffraction and Rietveld analysis; application to crystal-chemical studies of minerals at non-ambient conditions, *Eur. J. Mineral.*, 14, 241–249, 2002.
- Petrov, V. A., V. I. Vladimirov, and A. N. Orlov, A kinetic approach to fracture of solids, *Phys. Stat. Sol.*, 42, p. 197, 1970.
- Polyakov, A. I., About composition of the anomalous mantle of continental rift zones of Baikal and Eastern Africa, *Deep xenolites and lithosphere structure*, pp. 31–44, Nauka, Moscow, 1987.
- Pontecorvo, B., Neutron well logging – a new geological method based on nuclear physics, *Oil and Gas Journal*, 40, 32–33, 1941.
- Price, G. P., The photometric method in microstructural analysis, *Am. J. Sci.*, 273, 523–537, 1973.
- Pros, Z., Investigation of anisotropy of elastic properties of rocks on spherical samples at high hydrostatic pressures, *High pressure and temperature studies of physical properties of rocks and minerals*, 56 pp., Naukova Dumka, Kiev, 1977.
- Rais, J. R., *Earthquake focus mechanics*, 217 pp., Mir, Moscow, 1982.
- Rinaldi, R., G. Artioli, M. D. Dove, et al., Neutron scattering in mineral science, earth science, and related fields with the European spallation source (ESS), in *Scientific Trends in Condensed Matter Research and Instrumentation Opportunities at ESS*, Richter D., Ed., pp. 91–106, Progress Report ESS/SAC/Report 1/01, Forschungszentrum Julich, 2001.
- Roe, R. J., Description of crystallite in polycrystalline materials, General solution of pole figures inversion, *J. Appl. Phys.*, 36, (6), 2024–2031, 1965.
- Rochette, P., *J. Struct. Geol.*, 9, 1015, 1987.
- Sachs, G., Zur Ableitung einer Fließbedingung, *Z. Ver. Dtsch. Ing.*, 72, 734–736, 1928.
- Salganik, R. L., Mechanics of bodies with many cracks, *Izvestia Acad. Sci. USSR, MTT*, 4, 149–158, 1973.
- Sander, B., Zur Petrographisch-tektonischen Analyse, *Jahrb. Geol. Bundes Anstalt.*, A23, 215, 1923.
- Savelova, T. I., Functions of grain distribution by orientation and their Gaussian approximations, *Factory laboratory*, 50, (5), 48–52, 1984.
- Savelova, T. I., and T. I. Bukharova, *Presentation of group of SU(2) and their application*. MIFI, Moscow, 1996.
- Schäfer, W., Neutron diffraction applied to geological texture and stress analysis, *Eur. J. Miner.*, 14, 263–289, 2002.
- Schäfer, W., E. Jansen, R. Skowronek, et al., Setup and use of the ROTAX instrument at ISIS as angle-dispersive neutron powder and texture diffractometer, *Nucl. Instrum. Methods in Physics Research A.*, 364, 179–185, 1995.
- Scheffzük, Ch., A. Frischbutter, and K. Walther, Intracrystalline strain measurements with time-of-flight diffraction: Application to a Cretaceous sandstone from the Elbzone (Germany), *Schr. f. Geowiss.*, (6), 39–48, 1998.
- Schmidt, N.-H., and N. Ø. Olesen, *Canadian Miner.*, 27, 15–27, 1989.
- Shemyakin, E. I., Synthetic theory of strength, *Physical mezhomechanics*, 2, (6), 63–69, 1999.
- Shubnikov, A. V., *Piezoelectric textures*, 99 pp., Izd. Acad. Sci. USSR, M-L, 1946.
- Siegesmund, S., Fabric-controlled anisotropy of elastic, magnetic and thermal properties of rocks, in *Textures of geological materials* (edited by Bunge H.-J., Siegesmund S., Skrotzki W. and Weber K.), pp. 353–379, DGM special publication, 1994.
- Siegesmund, S., K. Ullemeyer, and M. Dahms, Control of rock magnetic fabrics by mica preferred orientation: a quantitative approach, *J. Struct. Geol.*, 17, 1601–1613, 1995.
- Siegesmund, S., A. Vollbrecht, K. Ullemeyer, T. Weiss, and R. Sobott, Application of geological fabric analysis for the characterization of natural building stones – case study Kauffung marble, *International Journal for Restoration of Buildings and Monuments*, 3, 269–292, 1997.
- Siegesmund, S., K. Ullemeyer, T. Weiss, and E. K. Tschegg, Physical weathering of marbles caused by anisotropic thermal expansion, *International Journal of Earth Sciences*, 89, 170–182, 2000.
- Siemens, H., H. Schaeben, C. A. Rosiere, and H. Quade, Crystallographic and magnetic preferred orientation of hematite in banded iron ores, *J. Struct. Geol.*, 22, 1747–1759, 2000.
- Silk, E. C., and R. S. Barnes, Examination of fission fragment track with an electron microscope, *Phil. Mag.*, 4, 970–971, 1959.
- Simmons, G., and H. Wang, *Single crystal elastic constants and calculated aggregate properties: a handbook*, Cambridge, Massachusetts, 370 p., 1971.
- Skrotzki, W., Mechanisms of texture development in rocks, *Textures of geological materials*, Informationsgesellschaft, Verlag, pp. 167–186, 1994.
- Sobolev, G. A., *Fundamentals of the earthquake forecast*, 312 pp., Nauka, Moscow, 1993.
- Sobolev, G. A., and V. N. Demin, *Mechanoelectric phenomena in the Earth*, 215 pp., Nauka, Moscow, 1980.
- Sobolev, G. A., and A. N. Nikitin, Neutronography in geophysics, *Physics of elementary particles and of atomic nucleus*, 32, (6), 1359–1404, 2001.
- Sobolev, G. A., A. N. Nikitin, T. I. Savelova, and V. B. Yakovlev, Experimentally-theoretic approach to investigation of micro- and macroproperties and state of rocks (feasible direction of development of the earthquake focus models), *Fizika Zemli*, (1), 6–15, 2001.
- Stavrogin, A. N., Investigation of limiting states and deformations of rocks, *Izvestia Acad. Sci. USSR. Fizika Zemli*, (12). 1969.
- Steinnes, E., *Epithermal neutron activation analysis of geological material, Activation analysis in geochemistry and cosmochemistry* (Brunfelt A. O., Steinnes E., eds.), Universitetsforlaget, pp. 113–128, Oslo, 1977.
- Taylor, G. I., Plastic strain in metals, *J. Inst. Met.*, 62, 307–324, 1938.
- Tectonophysics and mechanical properties of rocks*, 195 pp., Nauka, Moscow, 1971.
- Tuck, G., F. D. Stacy, and K. A. Starkey, A search for the piezoelectric effect in quartz-bearing rocks, *Tectonophysics*, 39, T17–T11, 1977.
- Ullemeyer, K., and K. Weber, Lattice preferred orientation as an indicator of a complex deformation history of rocks, *Textures and Microstructures*, 33, 45–60, 1999.
- Ullemeyer, K., P. Spalhoff, J. Heinitz J., et al., The SKAT texture diffractometer at the pulsed reactor IBR-2 at Dubna: experimental layout and first measurements, *Nucl. Instrument Meth. Phys. Res. A*, 412, (1), 1998.

- Ullemeyer, K., G. Braun, M. Dahms, et al., Texture analysis of a muscovite-bearing quartzite: a comparison of some currently used techniques, *Journal of Structural Geology*, 22, 1541–1557, 2000.
- Uyeda, S., M. D. Fuller, J. C. Belshe, and R. W. Girdler, Anisotropy of magnetic susceptibility of rocks and minerals, *J. Geophys. Res.*, 68, 279–291, 1963.
- Vaganov, P. A., *Neutron-activation investigation of geochemical associations of rare elements*, Nauka, Moscow, 1981.
- Viglin, A. S., Quantitative measure of texture of polycrystalline materials Texture function, *FTT*, 2, (10), 2463–2476, 1960.
- Volarovich, M. P., Mechanical properties of rocks at high pressures and their connection with porosity, *Present-day problems of the rock mechanics*, 250 pp., Leningrad. 1972.
- Volarovich, M. P., E. I. Bayuk, A. I. Levykin, and I. S. Tomashenskaya, *Physico-mechanical properties of rocks and minerals at high pressures and temperatures*, 222 pp., Nauka, Moscow, 1974.
- Volarovich, M. P., and E. I. Parkhomenko, Piezoelectric effect of rocks, *Dokl. Acad. Sci. USSR*, 90, (2), 239–242, 1954.
- Walther, K., A. N. Nikitin, V. Foitus, and T. I. Ivankina, Neutron diffraction investigation of texture properties of quartz rocks, *Izv. USSR Acad. of Sci., Fizika Zemli*, (11), 78–84, 1990.
- Walther, K., S. F. Kurtasov, A. N. Nikitin, and E. G. Torina, Simulation of deformation textures in high-temperature quartz, *Fizika Zemli*, (6), 45–48, 1993a.
- Walther, K., N. N. Isakov, A. N. Nikitin, K. Ullemeyer, and Y. Hainitz, Investigations of texture structure of geological materials by diffraction method with the help of the high resolution neutron spectrometer in the Frank Neutron physics laboratory of UINI, *Fizika Zemli*, (6), 37–44, 1993b.
- Whalley, E., D. W. Davidson, and J. B. R. Health, *J. Chem. Phys.*, 48, 2362, 1968.
- Walther, K., A. Frischbutter, and Ch. Scheffzük, Modernisation of the time-of-flight diffractometer EPSILON for strain measurements on geological samples, *II German-Russian User Meeting "Condensed Matter Physics with Neutrons at IBR-2"*, pp. 6–12, Dubna, April 21–25, 2001.
- Wasserman, G., and I. Greven, *Textures of metallic materials*, 653 pp., Metallurgia, Moscow, 1969.
- Wenk, H.-R., *Preferred orientation in deformed metals and rocks: An introduction to modern texture analysis*, 610 pp., FL: Academic Press, Orlando. 1985.
- Wenk, H.-R., H. Kern, W. Schaefer, and G. Will G, Comparison of neutron and X-ray diffraction in texture analysis of deformed carbonate rocks, *J. Struct. Geol.*, 6, 687–692, 1984.
- Wenk, H.-R., H. J. Bunge, E. Jansen, and J. Pannetier, Preferred orientation of plagioclase – Neutron diffraction and U-stage data, *Tectonophysics*, 126, 271–284, 1986.
- Wenk, H.-R., S. Matthies, and L. Lutterotti, Texture analysis from diffraction spectra, *Materials Science Forum*, 157–162, pp. 473–480, 1994.
- White, H., Geological significance of recovery and recrystallization processes in quartz, *Tectonophysics*, 39, 143–170, 1977.
- Widhalm, C., E. Tshegg, and W. Eppensteiner, Anisotropic thermal expansion causes deformation of marble cladding, *Journal of Performance of Constructed Facilities*, ASCE, 10, 5–10, 1996.
- Will, G., P. Merz, W. Schafer, and M. Dahms, Application of position sensitive detectors for neutron diffraction texture analysis of hematite ore, *Advanced in X-ray Analysis*, 33, 277–283, 1990.
- Young, D., Etching of radiation damage in lithium fluorid, *Nature*, 182, 357–377, 1958.
- Zhurkov, S. N., Kinetic concept of strength of solid bodies, *Vestnik Acad. Sci. USSR*, (3), 1968.
- A.N. Nikitin and T.I. Ivankina, Frank Laboratory of Neutron Physics Joint Institute of Nuclear Research Dubna, Moscow Region, 141980 Russia

(Received 11 August 2003)